EÜ GRADUATE SCHOOL OF NATURAL AND APPLIED SCIENCES

EGE UNIVERSITY

MASTER OF SCIENCE THESIS

INVESTIGATION OF THE INTERACTIONS OF THE PROMAZINE WITH SELECTED BIOMOLECULES USING PHOTOPHYSICAL AND COMPUTATIONAL METHODS

Tuğçe ŞENER

Supervisor: Assoc. Prof. Dr. Nursel ACAR SELÇUKİ

Department of Chemistry

Presentation Date : 08.08.2016

Bornova-İZMİR

2016

EGE UNIVERSITY GRADUATE SCHOOL OF NATURAL AND APPLIED SCIENCES

(MASTER OF SCIENCE THESIS)

INVESTIGATION OF THE INTERACTIONS OF THE PROMAZINE WITH SELECTED BIOMOLECULES USING PHOTOPHYSICAL AND COMPUTATIONAL METHODS

Tuğçe ŞENER

Supervisor: Assoc. Prof. Dr. Nursel ACAR SELÇUKİ

Department of Chemistry

Presentation Date :08.08.2016

Bornova-İZMİR

2016

Tuğçe ŞENER tarafından yüksek lisans tezi olarak sunulan "PROMAZİN MOLEKÜLÜNÜN SEÇİLMİŞ BİYOMOLEKÜLLERLE ETKİLEŞİMLERİNİN FOTOFİZİKSEL VE HESAPSAL YÖNTEMLERLE İNCELENMESİ" başlıklı bu çalışma EÜ Lisansüstü Eğitim ve Öğretim Yönetmeliği ile EÜ Fen Bilimleri Enstitüsü Eğitim ve Öğretim Yönergesi'nin ilgili hükümleri uyarınca tarafımızdan değerlendirilerek savunmaya değer bulunmuş ve 08.08.2016 tarihinde yapılan tez savunma sınavında aday oybirliği/oyçokluğu ile başarılı bulunmuştur.

Jüri Üyeleri: **İmza**

Jüri Başkanı :Doç. Dr. Nursel Acar Selçuki ….....

Raportör Üye :Doç. Dr. Armağan Kınal .....

Üye :Yard. Doç. Dr. Nilgün YENER .....

EGE ÜNİVERSİTESİ FEN BİLİMLERİ ENSTİTÜSÜ

ETİK KURALLARA UYGUNLUK BEYANI

EÜ Lisansüstü Eğitim ve Öğretim Yönetmeliğinin ilgili hükümleri uyarınca Yüksek Lisans Tezi olarak sunduğum "PROMAZİN MOLEKÜLÜNÜN SEÇİLMİŞ BİYOMOLEKÜLLERLE ETKİLEŞİMLERİNİN FOTOFİZİKSEL VE HESAPSAL YÖNTEMLERLE İNCELENMESİ" başlıklı bu tezin kendi çalışmam olduğunu, sunduğum tüm sonuç, doküman, bilgi ve belgeleri bizzat ve bu tez çalışması kapsamında elde ettiğimi, bu tez çalışmasıyla elde edilmeyen bütün bilgi ve yorumlara atıf yaptığımı ve bunları kaynaklar listesinde usulüne uygun olarak verdiğimi, tez çalışması ve yazımı sırasında patent ve telif haklarını ihlal edici bir davranışımın olmadığını, bu tezin herhangi bir bölümünü bu üniversite veya diğer bir üniversitede başka bir tez çalışması içinde sunmadığımı, bu tezin planlanmasından yazımına kadar bütün safhalarda bilimsel etik kurallarına uygun olarak davrandığımı ve aksinin ortaya çıkması durumunda her türlü yasal sonucu kabul edeceğimi beyan ederim.

.... / .... / 20..

İmzası

Tuğçe ŞENER

ÖZET

PROMAZİN MOLEKÜLÜNÜN SEÇİLMİŞ BİYOMOLEKÜLLERLE ETKİLEŞİMLERİNİN FOTOFİZİKSEL VE HESAPSAL YÖNTEMLERLE İNCELENMESİ

ŞENER, Tuğçe

Yüksek Lisans Tezi, Kimya Anabilim Dalı
Danışman: Doç. Dr. Nursel ACAR SELÇUKİ
Ağustos 2016, 83 sayfa

Bu tezde donör olarak seçilen biyomoleküller ile akseptör olarak seçilen promazin molekülü arasındaki yük transfer kompleksleri, fotofiziksel ve hesapsal yöntemler kullanılarak incelenmiştir.

Fenotiazin türevi olan promazin, antipsikotik veya nöroleptik ilaç olarak kullanılmaktadır. Ayrıca, fluoresans özelliğinden dolayı proteinlerin işaretlenmesinde biyosensör olarak da kullanılmaktadır. Promazin yapısındaki π-elektronik sistemleri nedeniyle absorpsiyon ve fluoresans özelliğe sahiptir ve temel halde bulunan ve azot atomu içeren bir biyomolekülle, donör-akseptör yük transfer kompleksleri oluşturabilir. Bu çalışmada, promazin ve hormonlar (dopamin, serotonin, melatonin) arasında oluşabilecek donör–akseptör sistemleri hem sağlık alanında ilaç tasarımında hem de modifiye nanomalzemelerin yapılmasında model olması amacıyla incelenmiştir. Seçilen bütün sistemlerin değişik polaritede hem deneysel hem de hesapsal incelemeleri yapılmıştır. Donör-akseptör kompleksleri arasında π-π etkileşimleri, dispersiyon kuvvetleri ve hidrojen bağları oluşumu beklenmektedir. Bu amaçla hesapsal olarak moleküller arasında oluşacak komplekslerin en kararlı geometrileri, dipol momentleri, Gibbs serbest enerji değerleri ve elektronik geçişleri belirlenmiştir. Deneysel olarak ise UV/Vis absorpsiyon spektrumları, fluoresans ölçümleri ve voltametrik ölçümleri yapılmıştır. Elde edilen sonuçlardan promazinin seçilen hormonlarla donor-akseptör yük transfer kompleksleri oluşturduğu görülmüştür.

Anahtar Kelimeler: Elektron Transferi, DFT (Yoğunluk Fonksiyoneli Teorisi), İlaç, Hormonlar, UV, Fluoresans

ABSTRACT

INVESTIGATION OF THE INTERACTIONS OF THE PROMAZINE WITH SELECTED BIOMOLECULES USING PHOTOPHYSICAL AND COMPUTATIONAL METHODS

ŞENER, Tuğçe

MSc in Chemistry
Supervisor: Assoc. Prof. Dr. Nursel ACAR SELÇUKİ
August 2016, 83 pages

In this thesis, intermolecular charge transfer complexes between the selected donor biomolecules with selected acceptor promazine have been investigated by photophysical and computational methods.

Promazine, a phenothiazine derivative, is used as a antipsychotic or a neuroleptic drug. Because of the presence of a π-electronic system in its structure, promazine shows fluorescence properties. It may form donor-acceptor electron transfer complexes with a ground-state biomolecule which has a nitrogen atom. Promazine will be used as the acceptor in this study. Donor molecules will be chosen among molecules which are naturally occurring or synthesized in human body with π-electronic systems and nitrogen atoms. π-π interactions, dispersive forces and hydrogen bond formation are expected between donor and acceptor in the formed complexes. Investigation of donor-acceptor complex formation between promazine and the hormones (dopamine, serotonin, melatonin) and determination of electron transfer mechanisms are important and will be a model for drug design studies and production of modified nanomaterials. Promazine is also used as a biosensor for marking proteins due to its fluorescence properties. All the systems will be investigated in different polarities using experimental and computational techniques. Most stable complexes will be determined computationally and their geometries, dipole moments, Gibbs free energies and their electronic transitions will be determined.

Keywords: Electron Transfer, DFT (Density Functional Theory), Drug, Hormones, UV, Fluorescence

ACKNOWLEDGEMENTS

This thesis becomes a reality with the kind help and support of many people. I would like to extend my sincere thanks to all of them.

In the first place, I would like to express the deepest gratitude to my advisor Assoc. Prof. Dr. Nursel Acar Selçuki for her full support, expert guidance, understanding, sharing her valuable knowledge with me and encouragement throughout my study and research. I would like to thank Assoc. Prof. Dr. Armağan Kınal for his support and help in Computational Chemistry and also for sharing his knowledge and expertise in this study. Also, I am grateful to Assoc. Prof. Dr. Cenk Selçuki for sharing his knowledge and technical information.

I wish to thank the department members at the Department of Chemistry for sharing, a friendly atmosphere; especially, to the members of the physical chemistry division for providing the worthy conditions and support throughout my studies.

I would like to thank my husband for giving the right advice at the right time and for being a source of motivation. I would like to thank and present my gratitude especially to my extended family.

TABLE OF CONTENTS

Page

TABLE OF CONTENTS (CONT.)

Page

TABLE OF CONTENTS (CONT.)

Page

LIST OF FIGURES

LIST OF FIGURES (CONT.)

LIST OF FIGURES (CONT.)

LIST OF TABLES

Table **Page**

LIST OF TABLES (CONT.)

Table **Page**

LIST OF SYMBOLS

Symbols	Description
S_0, S_1	Ground state and first singlet excited state of valence bond structures
P,R	Product, Reactanct
X	Transition state
E_a	Activation barrier
M^*	Electronically excited state of a molecule
Bi, Bt	Intensity of incident and transmitted beam
S	Scattering
L	Luminescence
A	Absorption
I	Isotropic photon density of radiation
A, B	Einstein coefficients
T_1	First triplet state
ν_a, ν_f	Transition energies of absorption and fluorescence
ε	Dielectric constant

n	Refractive index
A	Electron acceptor
D	Electron donor
χ , β	Coulomb and resonance integrals for carbon
ΔE_{CT}	Energy of charge transfer transition
$\bar{\upsilon}_A$, $\bar{\upsilon}_F$	Wave number of absorption and emission
h	Planck's constant
c	Speed of the light
a	Radius cavity of the fluorophore
R	Refractive field
f	Polarizability of the solvent
f(n)	Polarizability, a function of the refractive index
ΔG_{el}	Standard free energy change
Q	Quencher
[F]	The concentration of uncomplexed fluorophore
[Q]	The concentration of quencher

H	Hamiltonian operator of the Schrödinger Equation
ψ	Wave function
E	Total energy of the system
T_n	The kinetic energy of the nuclei
Te	Kinetic energy of electrons
V	Potential energy
N	Normalization constant
$Y_{l,m}$	Spherical harmonic functions.

Abbreviations

DAC	Donor acceptor complex
STO	Slater Type Orbitals
GTO	Gaussian Type Orbitals
DFT	Density Functional Theory
PAHs	Polycyclic Aromatic Hydrocarbons
DFT	Density Functional Theory
CNTs	Carbon Nanotubes
SWCNTs	Single-Walled Carbon Nanotubes
MWCNTs	Multi-Walled Carbon Nanotubes
PZ	Promazine

Abbreviations (Cont.)

DA	Dopamine
SE	Serotonin
MT	Melatonin
HOMO	Highest Occupied Molecular Orbital
LUMO	Lowest Unoccupied Molecular Orbital
LE	Locally Excited
CT	Charge transfer
DNA	Deoxyribo Nucleic Acid
OLED	Organic Light Emitting Diode

1. INTRODUCTION

Absorption of a photon in the visible or ultraviolet region is the essential step for the formation of an electronically-excited state in all photochemical and photophysical processes. Photochemical and photophysical processes are triggered by absorption of a photon.

Photophysically excited electron transfer processes play an important role in many scientific fields. A photophysically excited molecule is a better donor or acceptor compared to its ground-state form. This molecule causes chemical changes in neighboring ground-state molecule by electron transfer mechanism, thus making it photophysically sensitive. Charge transfer complexes and energy transfer processes formed by this mechanism play also important roles in biochemical processes.

One of the most important fields of excited state chemistry is complex formation in the excited state by charge transfer and it has been studied since 1955 (Förster et al, 1955; Leonhardt et al, 1961; Mataga et al, 1955). Other studies followed these pioneering studies as applications in photobiology, solar energy conversion, sensors and molecular electronic devices (Thrower, 2013; Shen, 2013; Nashed et al., 2013).

First studies related to electron transfer started about sixty years ago (Lippert, 1957; Mataga et al, 1956). Understanding the electron transfer mechanism will enable many fundamental and practical applications including photosynthesis, biological redox mechanisms and design of solar battery devices. Additionally, combination of experimental and theoretical data will provide useful information on producing molecular devices and designing new drugs.

Biologically important aromatic molecules like porphyrins, basic nucleotides, aromatic amino acids, some drugs have π-electron systems. The biochemical behavior of these molecules is affected by their photophysical properties which arise from the electronic excitation of these molecules by internal and external prosesses. Dopamine and serotonin act in the body as hormones and they are also neurotransmitters responsible for regulation of many fundamental processes in the brain like emotional state and control, sleep, awakeness, food intake and thermal stability (Takashi et al, 2004). On the other hand, melatonin, another hormone, regulates the biological clock. Its most

important function is to control many physiological and behavioral processes triggered by environmental light-darkness cycle (Harusuke et al, 1998). Promazine is a pyschotropic drug which is used extensively in mental disorders (Cogordan et al, 1999; Raghupathy et al, 1970; Pan et al, 1999) and anticancer activities (Wainwright et al, 2007; Nagy et al, 1996; Eghbal et al, 2004; Albery et al, 1979; Takada et al, 2006; Weiss et al, 2004; Kim et al, 2007; Imabayashi et al, 2003; Bloor et al, 1970; Takashi et al, 2004). Its interactions in metabolism with the chosen molecules (dopamine, serotonin and melatonin) are important in terms of its biological activity.

Since these molecules are biologically important, they were studied by different groups, mostly because of their pharmaceutical importance (Guo et al, 2009; Zafar et al, 2006; Mohammad-Shiri et al, 2011; Bernsmann et al, 2010; López Sastre et al, 2001; Chattopadhyay et al, 1996; Daniel et al, 1999; Daniel, 2003; Darvesh et al, 2013). Some studies also included some structural and chemical properties (Mohammad-Shiri et al, 2011; Bernsmann et al, 2010; López Sastre et al, 2001). Most recently these molecules began to attract attention for use in production of biocompatible materials (Bernsmann et al, 2010). These studies focused on single molecules and there are no reported studies on their intra or inter molecular complexes either in ground state or in excited state.

There are studies on intramolecular complex formation of promazine with some biomolecules in the literature; but, there are no reported studies on its intermolecular interactions. Stability of intermolecular complexes depends on total interaction energy (exchange, electrostatic and dispersive forces) because of π electrons (in some cases n electrons) between molecules.

The aim of this study is to understand charge transfer by light excitation of a photoactive components and modify the electronic interactions such as van der Waals forces and hydrogen bonding mechanisms as well as the factors affecting these processes between promazine and biologically important molecules dopamine, serotonin and melatonin.

In this study, intermolecular interactions between photophysically excited promazine and naturally occurring hormones (dopamine, serotonin, melatonin) in the human body at ground-state will be investigated using experimental and computational tools. Excitation of chromophoric systems and subsequent photochemical processes are still difficult to predict and to treat theoretically, even in some liquid phase. Therefore, the outcome of the work is important as it is

expected to gain detailed insight about donor-acceptor systems composed of organic-biological hybrid components. This information will provide useful information for many related fields including health, electronics, materials science etc.

1.1 The Interaction of Light with Matter

The interaction of light and matter either as a natural phenomenon or as an artificial process enters most branches of science, from medicine to material science (Turro et al, 2010; Klanp et al, 2009). Whole biological life depends on photosynthesis, a natural photochemical process. Many of most common functions exploited in our technological environment, from signal processing, storage and display to the use of pigments, sensors and sensitizers are based on light-matter interaction. Solar energy can be artificially converted into useful energy forms by photochemical and photophysical processes (Armaroli et al, 2011; Morristet al, 2009).

In some processes, electronic excitation can result in chemical changes: fading of dyes, photosynthesis in plants, suntans, or even degradation of molecules. As an alternative, the electronically-excited state may deactivate by a number of physical processes which may result either in emission of light (luminescence) or conversion of the excess energy into heat, and the original ground state is reformed. Energy-transfer or electron-transfer reactions may occur as a result of interactions between electronically-excited states and ground-state molecules, in case certain criteria are met.

The atoms in the material body have only two energy levels as a ground state M and an excited state M*. Excited states are formed by the absorption of radiation by ground states;

$$M + h\nu \rightarrow M^{*} \qquad (1.1)$$

and excited states can then decay back to the ground state through stimulated emission;

$$M^{*} \rightarrow M + h\nu \qquad (1.2)$$

The concentrations of ground and excited states of M be [M] and [M*] respectively and isotropic photon density of the radiation be I, then the kinetic equations are;

Absorption	d[M*] / dt = BI[M]	(1.3)
Spontaneous emission	d[M*] / dt = A[M*]	(1.4)
Stimulated emission	d[M*] / dt = -BI[M*]	(1.5)

In these equations A and B are known as Einstein coefficients which give the transition probabilities.

1.1.1 The transition moments

The Einstein coefficients are related to the quantity which describes the transition probability, known as the transition moment. During an electron transition, an electron jumps from one orbital to another. Its distance from the nucleus changes, so there is a change in the instantaneous dipole moment. The greater this change, the more probable the transition because it is the interaction between this transition dipole and the electric vector of light.

In an atom of spherical symmetry or a molecule which has an inversion centre there is no permanent dipole moment. They can have large transition moments, as these describe in effect the motion of an electron from one orbital to another. The overall symmetry is restored after electron jump.

1.1.2 The energy of light

In order of increasing energy, molecules have translational, rotational, vibrational and electronic excited states. The electronic excited states only lead to photochemistry, since their energies correspond to the frequencies of near IR, visible and near UV light. An electronic transition brings an atom or molecule from the ground state to one of its excited states, or vice versa.

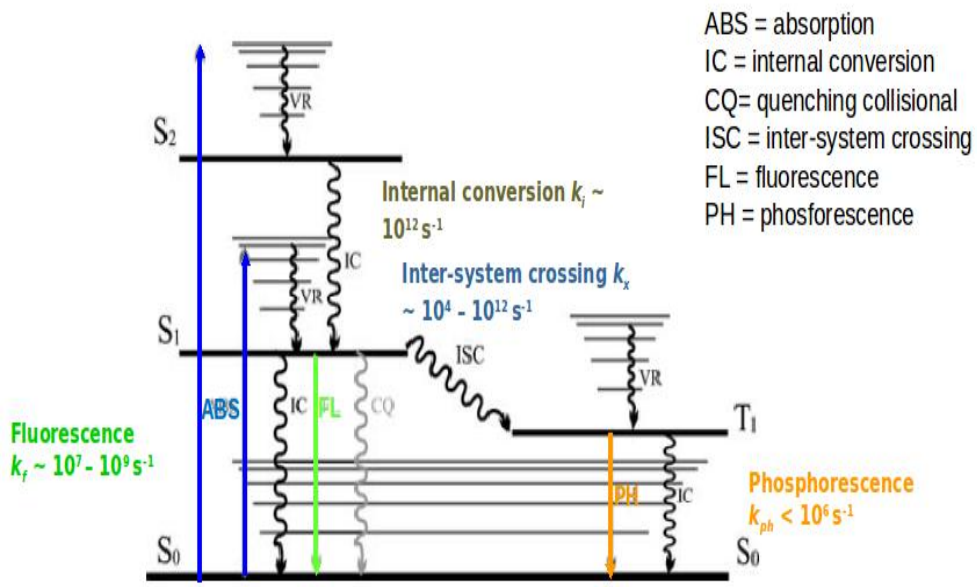

Figure 1.1. Jablonski diagram

The absorption and emission of light is nicely illustrated by the energy-level diagram suggested by A. Jablonski (Jablonski, 1933). A typical Jablonski diagram is given in figure 1.1. The singlet ground, first, and second electronic states are depicted by S_0, S_1, and S_2, respectively. At each electronic energy level, the fluorophores can exist in a number of vibrational energy levels. In this diagram, solvent effects are excluded. Vertical lines represent the transitions between different states to display the characteristics of light absorption. Transition occurs in a time scale of 10^{-15} s, a time too short for significant displacement of nuclei. This is the Franck-Condon principle (Onsager, 1931).

Light absorption is the initial step and is generally followed by many different processes. Usually, a fluorophore is excited to one of its higher S_1 or S_2 vibrational levels. Molecules in condensed phases mostly relax to the lowest S_1 vibrational level. The time interval for this process is around 10^{-12} s or less and the process is defined as internal conversion. Internal conversion usually ends before emission starts due to fluorescence lifetimes which are generally around 10^{-8} s. Fluorescence emission generally occurs from the lowest-energy vibrational S_1 state which is a thermally equilibrated excited state. Returning to the ground state usually occurs through a higher excited vibrational ground state level and then thermal equilibrium is reached very quickly in a time scale of 10^{-12} s.

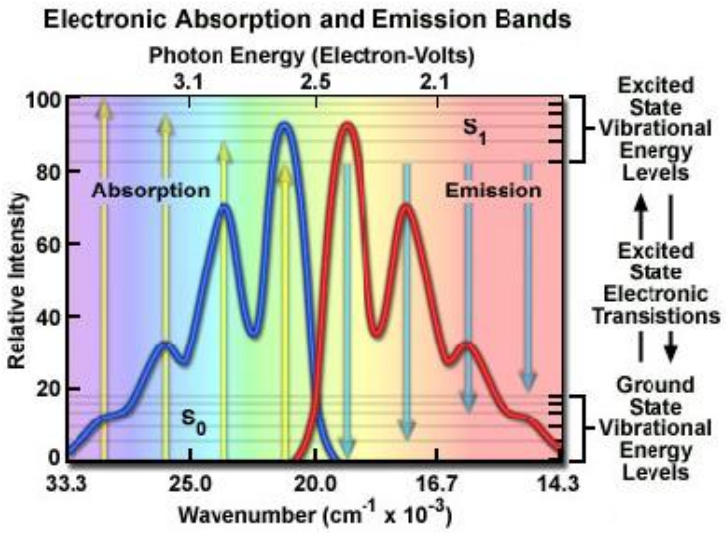

Figure 1.2. Electronic absorption and emission bands

In the emission to higher vibrational ground states, the emission spectrum is typically a mirror image of the absorption spectrum of the $S_0 \rightarrow S_1$ transition. This similarity occurs because nuclear geometry does not change much upon electronic excitation. As a result, vibrational energy levels in the excited and ground states are separated with the same amount of energy. Therefore, absorption and the emission vibrational structures observed in the absorption and the emission spectra resemble each other (figure 1.2).

An alternative process is the spin conversion of the molecules in the S_1 state to the first triplet state, T_1. Emission from T_1 is named phosphorescence and is generally shifted to longer wavelengths (lower energy) relative to the fluorescence. Conversion of S_1 to T_1 is called intersystem crossing. Transition from T_1 to the singlet ground state is forbidden, and, as a result, rate constants for triplet emission are several orders of magnitude smaller than those for fluorescence.

One of the important characteristics of fluorescence is that fluorescence emission spectra are generally independent from the excitation wavelength. This property is known as Kasha`s rule and was first reported by Vavilov in 1926 in terms of quantum yields. When excitation into higher electronic and vibrational levels occurs, the excess energy is lost immediately and the fluorophore remains in the lowest vibrational S_1 level. The time interval for this relaxation is around

10^{-12} s. Because of this fast relaxation, emission spectra are usually independent of the excitation wavelength.

Studies of the fluorescence and absorption spectra and other photo physical properties of aromatic molecules are performed in solution. The emitting or absorbing molecule is usulaay influenced by the surrounding solvent molecules which may cause significant changes in its photophysical properties. Thefore, the observed spectral and photophysical parameters are characteristic of the molecule in its solvent environment rather than of the isolated molecule.

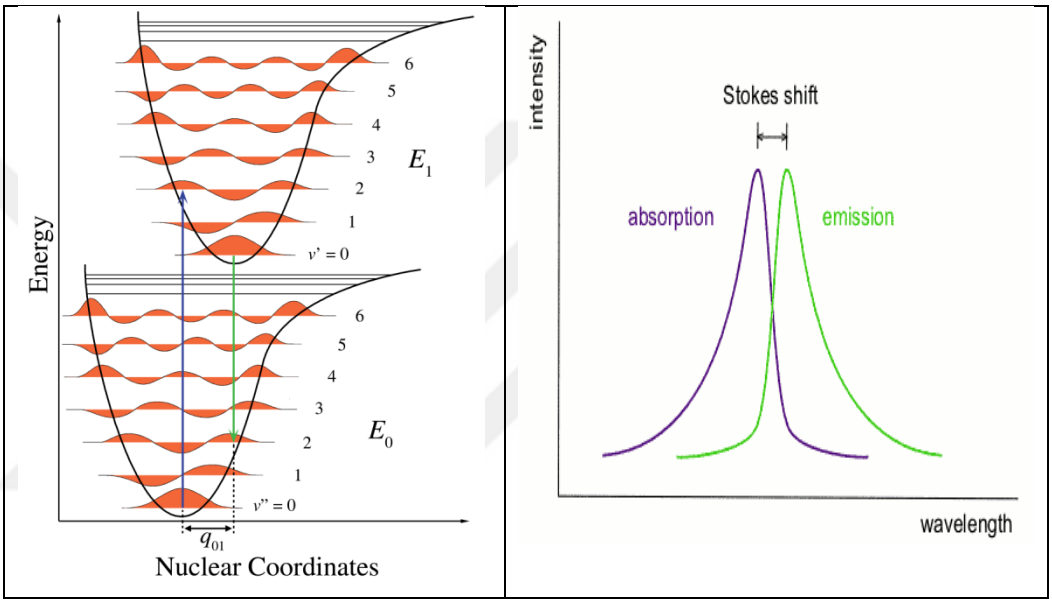

Figure 1.3. Potential energy

In solution each of the spectral parameters is normally shifted to lower energies, and the 0-0 transitions no longer coincide (figure 1.3.). As a result, $\Delta\nu_A - \Delta\nu_F > 0$, where ν_A and ν_F represent the transitions energies of absorption and fluorescence, respectively. There are two types of intermolecular interaction responsible for the spectral changes in a solvent medium: general and specific solvent effects. A general solvent effect (universal interaction) arises from the dielectric constant (ε) and the refractive index (n). These physical constants reflect the degree of motional freedom of the electrons in the solvent molecules, and the dipole moments of the molecules. The spectral changes due to universal interactions are described in terms of the Onsager theory of dielectrics (Lakowicz, 1999) and the Franck-Condon principle (Franck, 1926). Specific solvent effects refer to specific chemical interactions between the fluorophore and the solvent

molecules, such as the formation of hydrogen bonds, complexes or exciplexes. Both general and specific solvent interactions can result in significant spectral shifts. General solvent effects are always expected to be present. In contrast, specific solvent effects will depend upon the precise chemical structures of the solvent and solute.

Polarity sensitive spectral changes of polyaromatic hydrocarbons results from interactions of the dipole moment of the excited fluorophore with reactive fields induced in the surrounding solvents, and from hydrogen bonding between the fluorophore and solvent molecules. The dipole moments of the electronically excited compounds are larger than those of the corresponding ground state species. This situation perturbs the solute-solvent structure and the lifetime of the first excited state changes depending on the solvent polarity (Lakowicz, 1999).

In non-polar solvents the quenching of the fluorescence of aromatic electron donors (D) by electron acceptors (A) is usually associated with the formation of an intermediate exciplex $^{1}(A^{-}D^{+})^{*}$, characterized by a new fluorescent band. The use of methods based on nanosecond laser photolysis has been the main approach for measuıring the absorption spectra of several exciplexes (Potashnik et al, 1971). In polar solvents such as methanol or acetonitrile, the exciplex emission is extremely weak and the corresponding absorption is replaced by that of the relatively long lived ionic dissociation products A^{-}_{s} and D^{+}_{s}. The systems formed by the increasing solvent polarity effects were investigated formerly (Orbach et al, 1975; Kuzmin, 1993; Knibbe et al, 1967).

1.2 Excited States of Molecules

1.2.1 Diatomic molecules

In a very simple molecule such as hydrogen, two H atoms come together to form a chemical bond. The two atomic orbitals interact when they are very close each other. And this interaction can lead to two opposite situations, as shown in figure 1.4.

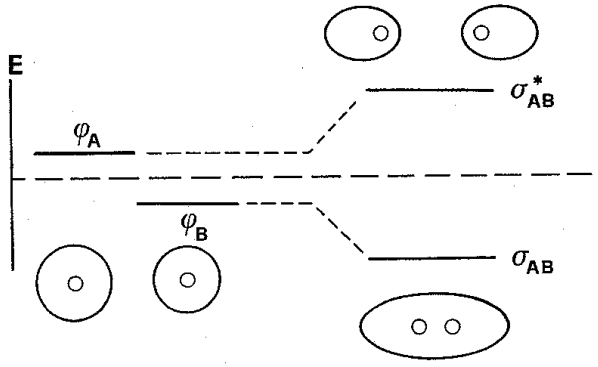

Figure 1.4. The interaction of two atomic orbitals leads to the formation of bonding and antibonding molecular orbitals of different energies.

A bonding molecular orbital is formed if two electrons are found in the space between the nuclei; they provide a shield between the two positively charged protons so that their electrostatic repulsion is lowered. An antibonding molecular orbital is formed if the two electrons are localized outside the internuclear region, so that the repulsion of the nuclei is actually greater than in the case of two separate atoms at the same distance. The energies of the bonding and antibonding orbitals are therefore lower and higher, respectively, than that of the constituent atomic orbitals.

Two orbitals play a special role and are known as "Highest Occupied Molecular Orbital (HOMO)" and the Lowest Unoccupied Molecular Orbital (LUMO)", these labels are referring of course to the situation in the ground state. The transition of an electron between these orbitals corresponds to the lowest excited state(s), e.g. triplet T_1 and singlet S_1.

1.2.2 Aromatic molecules

The benzene molecule is the simplest representative of a very large family of cyclic conjugated molecules. Aromatic molecules are formed essentially through the substitution, linking and fusion of the benzene ring which consists of six carbon atoms linked in a hexagonal cycle. Since there are six p orbitals which interact to form the molecular orbitals, there will be three bonding π orbitals and three antibonding π^* orbitals.

1.2.3 Electronic transition types

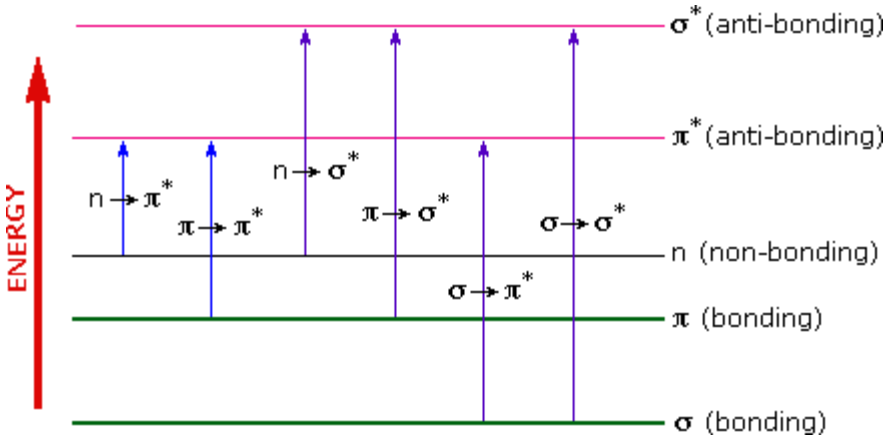

Figure 1.5. Energy diagram of transitions

Some typical transitions are presented in figure 1.5.

In **σ–σ* transitions,** excitation occurs from a bonding s orbital to the corresponding antibonding orbital. This process requires large amounts of energy. The most common example is methane as it has only C-H bonds, and can only undergo σ–σ* transitions. Its absorbance maximum is at 125 nm. Because of low wavelength values, absorption maxima of σ–σ* transitions are not observed in typical UV-Vis. spectra which cover 200 - 700 nm range.

n–σ* transitions are observed in saturated compounds with lone pairs (non-bonding electrons) on atoms. These transitions usually require less energy compared to σ–σ* transitions. The initiation for this process requires light in 150 - 250 nm range. There are only a few organic functional groups with n–σ* peaks in the UV region.

The main transitions in absorption spectroscopy of organic compounds are **n-π* and π-π* transitions**. The importance of these transitions comes from their absorption peaks for the transitions which fall in the experimentally detectable spectral region between 200 and 700 nm. An unsaturated group in the molecule which provides the p/π electrons is required.

n→π* absorption is a characteristic of molecules which have chromophores with multiply bonded hetero-atoms (e.g. C=O, C=N, C=S, N=N, N=O). It has low intensity ($f \approx 10^{-2} - 10^{-4}$) as it is symmetry or overlap forbidden. It is normally the band occurring at the wavelength. n-π* transitions have relatively lower molar absorbtivities within the range of 10 -100 L mol^{-1} cm^{-1}whereas π-π* transitions have molar absorbtivities within the range of 1000 - 10,000 L mol^{-1} cm^{-1}.

The medium, especially, the solvent in which the absorbtion takes place affects the spectra. The peaks for n-π* transitions shifted to shorter wavelengths (blue shift) with increasing solvent polarity. The energy of the n orbital is lowered by the increased solvation of the lone pair. On the contrary, π-π* transitions often show an opposite trend and display red shift. The main reason for this behavior is the attractive polarisation forces between the solvent and the absorber. These forces lower the energy levels of both excited and unexcited states. The energy change is larger for the excited state and the energy difference between the excited and unexcited states becomes smaller and causes a red shift. A similar effect is present in n-π* transitions but the main process is the blue shift caused by the solvation of lone pairs which dominates over this red shift.

Charge-transfer (CT) transitions

Charge-transfer complexes are characterized by charge-transfer absorption. These complexes must have two components: an electron donor and an electron acceptor. Charge transfer process involves the transfer of an electron from the donor to the acceptor by absorption of radiation.

Molar absorbtivities from charge-transfer absorption are large (greater that 10,000 L $mol^{-1}cm^{-1}$). Mixing electron donors and electron acceptors in solution often forms a new absorption band. This new band does not carry properties of its components. It is attributed to the presence of a donor acceptor complex (DAC) in those mixtures. This transition is referred to as a charge transfer (CT) transition and generally is broad and structureless. The nature of the bonding in DACs and the theory of CT absorption have been worked out by Mulliken (Mulliken, 1952). The ground state of A DAC is described by a wavefunction:

$$\psi_{(S_0)} = a\psi_{(DA)} + b\psi_{(D^+A^-)} \qquad (1.1)$$

In which $\psi_{(DA)}$ corresponds to a `no-bond` structure, the components being held only by weak intermolecular forces such as hydrogen bonding and dipole-dipole interaction and $\psi_{(D^+A^-)}$ corresponds to the structure in which an electron has been totally transferred from the donor to the acceptor. The wavefunction for the excited states of the DAC is then diven by;

$$\psi_{(S_1)} = a\psi_{(D^+A^-)} - b\psi_{(DA)} \qquad (1.2)$$

In general, b << a, so that $\psi_{(S_0)}$ ~ $\psi_{(DA)}$ and $\psi_{(S_1)}$ ~ $\psi_{(D^+A^-)}$. Thus, the spectroscopic transition corresponds approximately to the light induced transfer of an electron from the donor to the acceptor, and is named charge-transfer transition. It is observerd that there is very little charge-transfer in the ground state.

The energetics of DACs can be explored with energy diagrams. In figure 2.6, ΔH_0 and ΔH_1 are the energies of formation of the ground state of DAC from D and A, and the excited state from D^+ and A^-, and A_A and I_D are the electron affinity of the acceptor and the ionization potential of the donor. The energy of the CT transition (ΔE_{CT}) is written by;

$$\Delta E_{CT} = I_D - A_A - (\Delta H_1 - \Delta H_0) \qquad (1.3)$$

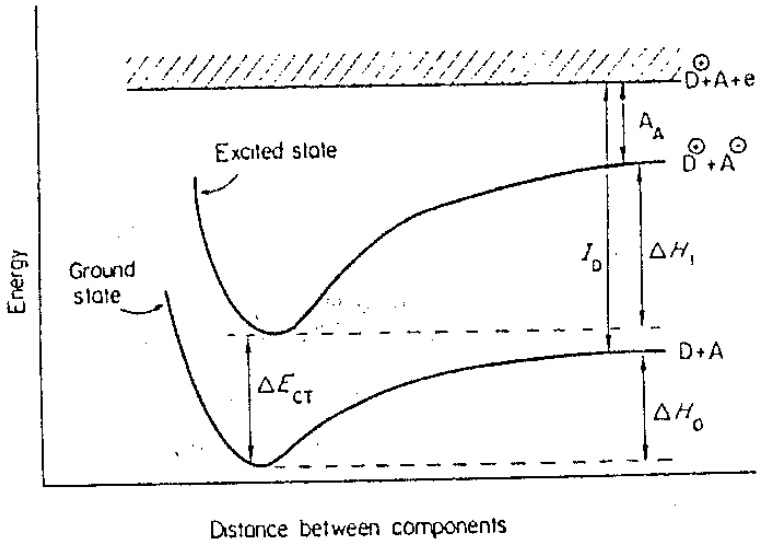

Figure 1.6. Energetics of donor-acceptor complexes.

1.3 The Reactions of the Electronically Excited Molecules

In order to follow the reaction by fluorescence measurements, the reaction time must be comparable to or shorter than the mean lifetime of the excited molecules. The reactions of the electronically excited molecules can be classified as follows (Weller, 1961).

1.3.1 Quenching of fluorescence (probably electron transfer)

An excited molecule, A*, loses its energy through interaction with molecule B instead of fluorescence radiation.

$$A^* + B \rightarrow (A^{(\pm)}.B^{(\pm)} \rightarrow) A + B \qquad (1.4)$$

1.3.2 Complex formation

An excited form of molecule, A*, can undergo complex formation either with the same molecule in ground state, A, or with another molecule, in ground state, B

$$A^* + A \rightarrow A^*A \qquad (1.5)$$

$$A^* + B \rightarrow A^*B \qquad (1.6)$$

1.3.3 Acid base reactions

The acid-base reactions can proceed as follows;

$$A^*H + B \rightarrow A^* + HB^+ \qquad (1.7)$$

$$A + HB \rightarrow AH^+ + B^- \qquad (1.8)$$

1.4 Thermodynamic Investigation

1.4.1 Solvent effects on emission spectra

Emission from fluorophores generally occurs at longer wavelengths than those at which absorption occurs. This loss of energy is due to dynamic processes which occur following light absorption (figure 1.7).

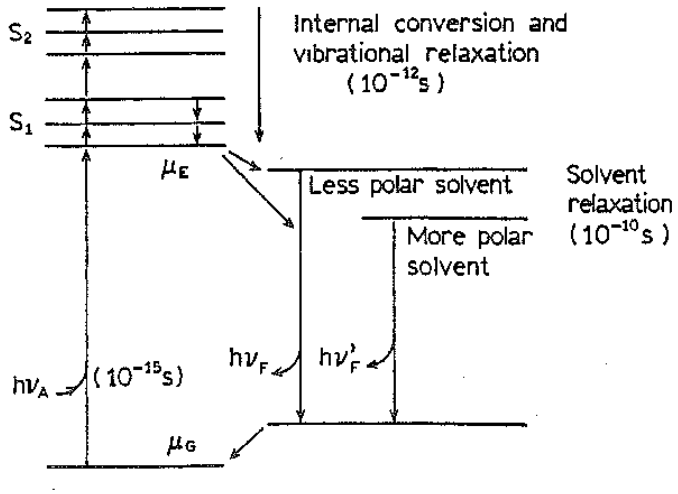

Figure 1.7. Jablonki diagram for fluorescence with solvent relaxation.

On the other hand, fluorescence lifetimes are usually longer than the time for solvent relaxation so that the emission spectra are pattern of the solvent relaxation. But absorption of light occurs in about 10^{-15} s. This time is too short for motion of the fluorophore or solvent and this can explain why the absorption spectra are less sensitive to solvent polarity than emission spectra.

1.4.2 Rehm Weller equation

Having established thermodynamic relationships for deriving the electromotive forces of reductions and oxidations of excited-state donor and acceptor molecules and calculating the free-energy change accompanying excited-states electron transfer, a useful expression is given figure 1.8.

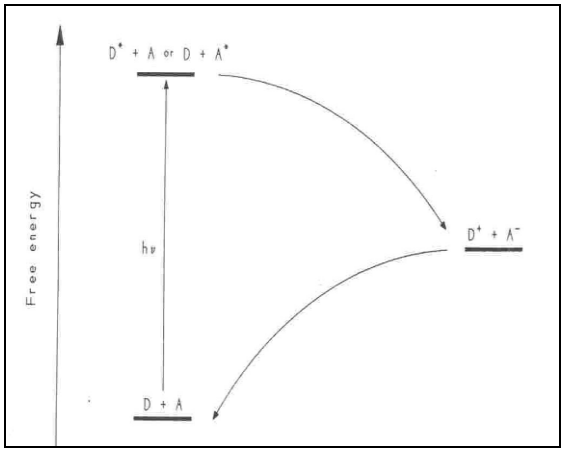

Figure 1.8. Energy diagram for photoinduced electron transfer

The total free-energy change for the uphill process is equal to the sum of the free-energy changes for oxidation of the donor and reduction of the acceptor;

$$\Delta G_{el} = \Delta G_{D/D}^{+} + \Delta G_{A/A}^{-} \quad (1.9)$$

In this equation, ΔG_{el} is the standart free-energy change.

$$\Delta G_{el}(eV) = nF(-E_{D/D}^{+} - E_{A/A}^{-}) \quad (1.10)$$

It can be written by using all half-reactions as reductions and redox potentials,

$$\Delta G_{el}(eV) = nF[E^{o}(D^{+}/D) - E^{o}(A/A^{-})] \quad (1.11)$$

The free-energy change when an electron transfer occurs between an excited donor and ground-state acceptor. It is called the thermodynamically downhill reaction and can be derived,

$$\Delta G_{el}(eV) = nF[E^{o}(D^{+}/D^{*}) - E^{o}(A/A^{-})] \quad (1.12)$$

and $\Delta G_{el}(eV)$ can be written like,

$$\Delta G_{el}(eV) = nF[E^{o}(D^{+}/D) - E^{o}(A/A^{-}) - \Delta G_{00}] \quad (1.13)$$

where ΔG_{00} is the free energy in electron volts corresponding to the equilibrium energy E_{00}. For one electron transfers nF is nearly equal to 1, so Eq. [1.13] can be written,

$$\Delta G_{el}(eV) = E^{o}(D^{+}/D) - E^{o}(A/A^{-}) - \Delta G_{00} \quad (1.14)$$

If the excited-state energy measures in kilocalories per mole and redox potentials in volts, Eq. [1.14] can be written as,

$$\Delta G_{el}(kcal\ mol^{-1}) = 23.06[E^{o}(D^{+}/D) - E^{o}(A/A^{-})] - \Delta G_{00} \quad (1.15)$$

There is an important revision in Eq. [1.15]. Assume that the donor and acceptor are neutral molecules. Electron transfer occurs, two charged species $-D^{+}$ and $-A^{-}$ are generated. This ion pair is formed by attractive Coulombic forces. These forces put together the two ions and as a result, the energy is released. This attraction is given by, w_p, derived from Coulomb´s law.

$$w_p(kcalmol^{-1}) = \frac{(z_d{}^{+} z_a{}^{-})e^2}{d_{cc}e_s} = \frac{332(z_d{}^{+} z_a{}^{-})}{d_{cc}e_s} \quad (1.16)$$

Where $z_D{}^{+}$ and $z_A{}^{-}$ are the charges on the molecules, e_s is the static dielectric constant of solvent, and d_{cc} is the center-to-center separation distance in Angstroms ($\overset{0}{A}$) between the two ions. Combining Eq. [1.13] and Eq. [1.16] gives,

$$\Delta G_{el}(\text{kcal mol}^{-1}) = 23.06[E^o(D^+/D) - E^o(A/A^-)] - w_p - \Delta G_{00} \quad (1.17)$$

which is called the Rehm-Weller equation. Equation [1.17] is more important for photochemistry and this is the fundamental thermodynamic condition for spontaneous electron transfer between neutral reactants: $\Delta G_{el}<0$ (Kavarnos, 1993).

1.5 Quenching of Excited States

Quenching is the non-radiative deactivation of an excited molecule M^* by a molecule Q (the quencher). The excited state energy eventually becomes heat energy of the surroundings (e.g. liquid solvent or solid matrix).

$$M^* + Q \rightarrow M + Q \ (+\text{energy}) \quad (1.18)$$

Quenching could be defined as the catalytic deactivation of excited molecules without chemical reaction. It will be used for the definition of quenching in photophysical process in which the molecule M^* is restored unchanged to its ground state M. A variety of processes can result in quenching. These include excited state reactions, energy transfer, complex formation, and collisional quenching. Both static and dynamic quenching require molecular contact between the fluorophore and quencher. In the case of collisional quenching, the quencher must diffuse to the fluorophore during the lifetime of the excited state. Upon contact, the fluorophore returns to the ground state without emission of a photon. The magnitude of fluorescence quenching depends on both acceptor and solvent.

Quenching measurements can reveal the accessibility of fluorophores to quenchers. If a given solvent is very viscous, then diffusion is slow and quenching is inhibited. Hence, quenching can reveal the diffusion rates of quenchers. Furthermore, fluorescence efficiency can be lower with increasing acceptor concentration.

Fluorescence quenching has been descried by Stern-Volmer Equation. Considering the ratio of the quantum yields;

$$\Phi_Q = \frac{k_r}{\sum k_i + k_q[Q]} \tag{1.19}$$

with the rate constant k_1 and using Equation (1.19) yield;

$$\frac{\Phi_f}{\Phi_Q} = \frac{\sum k_i + k_q[Q]}{\sum k_i} = 1 + k_q[Q]\tau_0 \tag{1.20}$$

where [Q] is the quencher concentration Instead of quantum yields, the fluorescent intensities in the absence (I_f) and presence quencher (I_Q) be written Taking into account dynamic quenching constant

$$K_{SV} = k_q\, \tau_0 \tag{1.21}$$

and hence reforming Equation [1.21] give;

$$\frac{I_f}{I_Q} = 1 + K_{sv}[Q] \tag{1.22}$$

which is the Stern-Volmer Equation The graph drawn between $\left[(I_f / I_Q) - 1\right]$ and $[Q]$ gives a straight line with the slope K_{sv} and substitution the actual fluorescence lifetime for τ_0 gives the rate constant k_q.

If complex formation between donor and acceptor in charge-transfer transition interaction takes place in the excited state not in the ground state this complex is named as “Exciplex” and the corresponding band can be seen in emission spectrum (Leonhardt, H. and Weller, 1961).

1.6 Electron and Energy Transfer

When the concentration of a solute is increased, it is commonly observed that there is a decrease in its fluorescence intensity. This is called concentration quenching. It has been found that such quenching is accompanied by the appearance of a new emission at longer wavelengths and the intensity of this band is increased with concentration. For example, the violet fluorescence of pyrene in dilute solution is replaced by a blue fluorescence with increasing pyrene concentration. Förster and Kasper showed that these phenomena could be

explained by the formation and fluorescence of a pyrene excimer (Monzon et al, 2008).

Many aromatic hydrocarbons and derivatives exhibit a second type of fluorescence in concentrated solution, known as excimer fluorescence (Förster et al, 1955). Benzene, naphthalene and their methyl derivatives are the other examples of excimer systems.

If two molecules form a complex in the excited state, it is called as exciplex (excited complex). These types of complexes form because of the diffusional quenching of two molecules and called encounter complexes. As a result, the charge distribution shifts from the donor molecule to the acceptor and this process is called the intermolecular electron transfer.

Exciplexes with a close charge separation can be explained as localized positive charge on donor and localized negative charge on acceptor (β>α). Charge separation has been observed by the nonradiative transition or emission (exciplex fluorescence) in nonpolar solvents. It can be usually separated in solvated radical ion forms in more polar solvents.

Exciplexes may be deactivated by another ground-state molecule, and it has been suggested that electron transfer may play a role in this deactivation (where A* is an excited acceptor and D is a donor).

$$A^* + D \leftrightarrow \left[A^* - D\right] \rightarrow A^{-\cdot} + D + D^{+\cdot} \qquad (1.23)$$

A photoexcited molecule may react with a ground-state molecule to undergo electron transfer at an encounter distance yielding a radical ion pair in polar media.

$$A^* + D \xrightarrow{acetonitrile} A^{-\cdot} + D^{+\cdot} \qquad (1.24)$$

In order to convert light energy into chemical energy in an efficient manner, the rate of reverse electron transfer must be controlled or stopped.

2. COMPUTATIONAL THEORY

Chemistry has been known as an experimental science and no molecule could be investigated until it was synthesized or found in nature. Computational chemistry has allowed scientists to predict the structures, energies, and other properties of molecules by calculations. The major difference between the experimental and computational techniques is that calculations can be performed easily for compounds that have never been synthesized, or even do not exist under normal conditions. One can calculate molecular structure, heat of formation, dipole moment, ionization potentials, charge densities, etc. in a single process which is impossible to determine in one experiment.

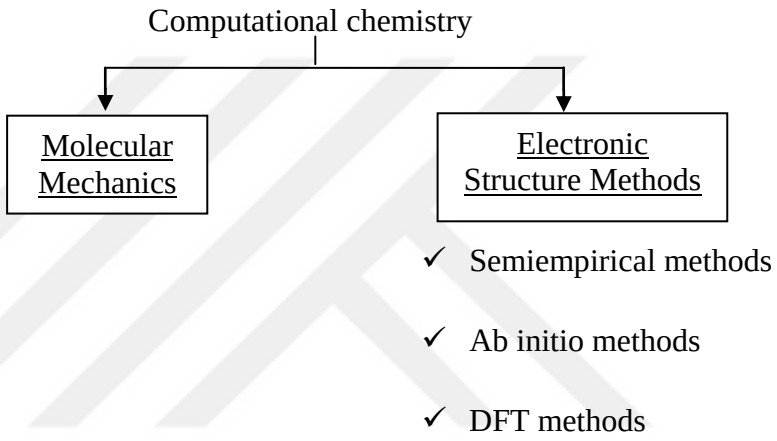

The computational methods are classified in two main groups: force field or molecular mechanics calculations and electronic structure methods. Electronic structure methods also consist of semiempirical methods, ab initio and DFT methods.

2.1 Molecular Mechanics Methods

Molecular mechanics methods are based on classical physics. There are many different molecular mechanics methods which are characterized by its particular force field. This method performs calculations depending on the nuclear interactions, implicitly taking electrons into account. This approximation makes molecular mechanics computations very fast and they are useful for very large systems.

2.2 Electronic Structure Methods

Electronic structure methods use the laws of quantum mechanics for their computations. Wavefunctions are used to describe the state of a system in quantum mechanics and they are donated by ψ. The wavefunction depends only on the spatial coordinates of the system and time. The properties of a system are usually time independent or time averaged. For a complete description of an atom, the Schrödinger Equation which includes the relations of the electrons with the nucleus among themselves is used

$$H \psi = E \psi \tag{2.1}$$

H= Hamiltonian operator of the Schrödinger Equation

ψ = wavefunction

E = total energy of the system

The Hamiltonian operator is used to calculate energies (eigenvalues) and the wave function which is an eigenfunction of the operator H.

For any but the smallest systems, however, exact solutions to the Schrödinger equation are not computationally practical. Electronic structure methods are characterized by their various mathematical approximations to its solution. Born–Oppenheimer is one of the approximations where the coupling between the nuclei and electronic motion is neglected. Electron move faster with respect to the nuclei which have larger mass; so, nuclei can see an averaged potential of electrons whereas electrons can see any positional change in nuclei. It can be separated into nuclear and electronic wavefunction as in the equation.

$$H = T_n + T_e + V \tag{2.2}$$

$$\Psi = \Psi_n + \Psi_e \tag{2.3}$$

Hamiltonian is shown in Eq.(2.3). T_n denotes the kinetic energy of the nuclei, T_e stands for the kinetic energy of the electrons and V represents the potential energy. The nuclei move slower than the electrons, the kinetic energy of the nuclei can be neglected and the repulsion between the nuclei can be considered to be constant during the optimization (Born-Oppenheimer approximation) (Levine, 1991).

2.2.1 Semiempirical methods

Semiempirical methods are characterized by use of parameters derived from either experimental or high quality computational data in order to simplify the approximation to the Schrödinger Equation. As parameters are used instead of expensive integrals in the calculations, semiempirical methods are relatively inexpensive and can be practically applied to very large molecules. The most commonly used methods in this group are AM1 and PM3.

2.2.2 Ab initio methods

Ab initio methods solve the Schrödinger equation without using parameters. In reality, *ab initio* methods also make use of experimental data with a different approach. Many different approximate methods exist for solving the Schrödinger equation. The choice of the method to use for a specific problem is usually based on the comparison of the performances with the available experimental data. Experimental data is used in the *selection* of the computational model, rather than in the computational procedure.

Use of a basis set is one of the most important approximations in *ab initio* approach. If a complete basis set is used, an unknown function, such as a molecular orbital, in a set of known functions can be accurately described. Unfortunatley, a complete basis set means use of an infinite number of functions and is not realistic. Instead, a finite basis set is used where the MO is represented by the selected basis functions. The size of the basis set and the *type* of basis functions used influence the accuracy.

There are two types of basis functions commonly used in electronic structure calculations: *Slater Type Orbitals* (STO) and *Gaussian Type Orbitals* (GTO).

Slater type orbitals have the functional form shown in Eq (2.4).

$$\chi_{\zeta,n,l,m}(r,\theta,\phi) \propto Y_{l,m}(\theta,\phi)\, r^{n-1} e^{-\zeta r} \qquad (2.4)$$

Here N is a normalization constant and $Y_{l,m}$ are spherical harmonic functions. The exponential dependence on the distance between the nucleus and electron mirrors the exact orbitals for the hydrogen atom. STO describes fairly well the radial electron distribution. However, STO is difficult to handle because integrations can not be calculated analytically.

Gaussian type orbitals can be written in terms of polar or Cartesian coordinates as shown in eq (2.5)

$$\chi_{\zeta,n,l,m}(r,\theta,\phi) \propto Y_{l,m}(\theta,\phi)\, r^{2n-2-l} e^{-\zeta r2} \qquad (2.5)$$

GTO describes less satisfactorily the radial electron distribution. However, GTO is easy to handle because integrations can be calculated analytically.

2.2.3 Density functional methods

The basis for Density Functional Theory (DFT) is the proof by Hohenberg and Kohn [45] that the ground state electronic energy is determined completely by the electron density ρ (Kohn et al,1965).

The significance of the Hohenberg–Kohn theorem is perhaps best illustrated by comparing it with the wavefunction approach. A wavefunction for an N electron system contains $4N$ variables, three spatial and one spin coordinate for each electron.The electron density is the square of the wave function, integrated over $N - 1$ electron coordinates, and each spin density only depends on three spatial coordinates, independent of the number of electrons. While the complexity of a wavefunction increases exponentially with the number of electrons, the electron density has the same number of variables, independent of the system size. The goal of DFT methods is to design functionals connecting the electron density with the energy. A wavefunction and the electron density are thus functions, while the energy depending on a wavefunction or an electron density is a functional. We will denote a function depending on a set of variables with parenthesis, $f(\mathbf{x})$, while a functional depending on a function is denoted with brackets, $F[f]$.

Early attempts at developing DFT models (actually predating wave mechanics) tried to express all the energy components as a functional of the electron density but these methods had poor performance, and wavefunction-based methods were consequently preferred. The success of modern DFT methods is based on the suggestion by Kohn and Sham in 1965 that the electron kinetic energy should be calculated from an auxiliary set of orbitals used for representing the electron density. The exchange–correlation energy, which is a rather small fraction of the total energy, is then the only unknown functional, and even relatively crude approximations for this term provide quite accurate computational models. The simplest model is the local density approximation, where the electron density is assumed to be slowly varying, such that the exchange–correlation

energy can be calculated using formulas derived for a uniform electron density. A significant improvement in the accuracy can be obtained by making the exchange–correlation functional dependent also on the first derivative of the density, and further refinements also add the second derivative and mix Hartree–Fock exchange into the functional. Density functional theory is conceptually and computationally very similar to Hartree–Fock theory, but provides much better results and has consequently become a very popular method.

3. EXPERIMENTAL

3.1 Apparatus

The following methods were used for the investigation of absorption and emission spectra. Preliminarily the donor and acceptor solutions were optimized by recording the absorption and emission data at λ_{max} for a series of selected donor and acceptor solutions in varying concentrations.

3.1.1 UV-Vis Spectroscopy

All the absorbance measurements were taken using Perkin Elmer UV visible Spectrophotometer. The thickness of quartz cuvette is 1 cm.

3.1.2 Steady-state fluorescence spectroscopy

Steady-state measurements were performed by RF-5301PC Spectrofluorophotometer Shimadzu. During measurements of fluorescence intensities and lifetimes, nitrogen gas was applied to remove the dissolved oxygen in the solution so that the quenching effect due to presence of oxygen was disappeared (figure 3.1).

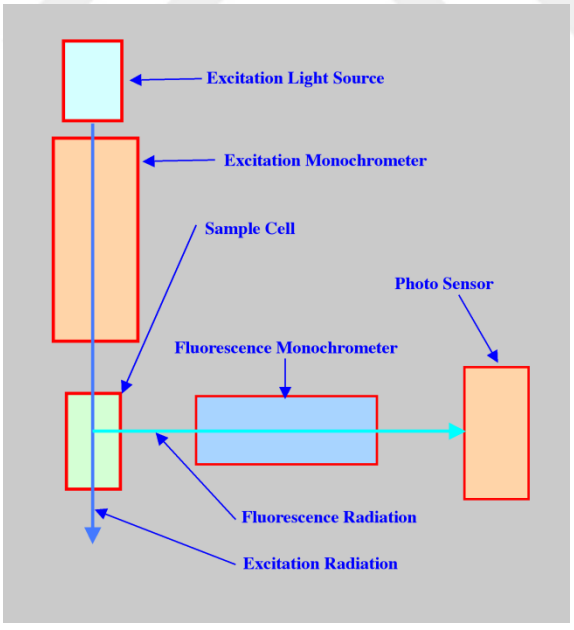

Figure 3.1. Steady state fluorescence spectroscopy

3.1.3 Reagents and solutions

Molecular structures of the studied molecules are shown in Figure 3.2.

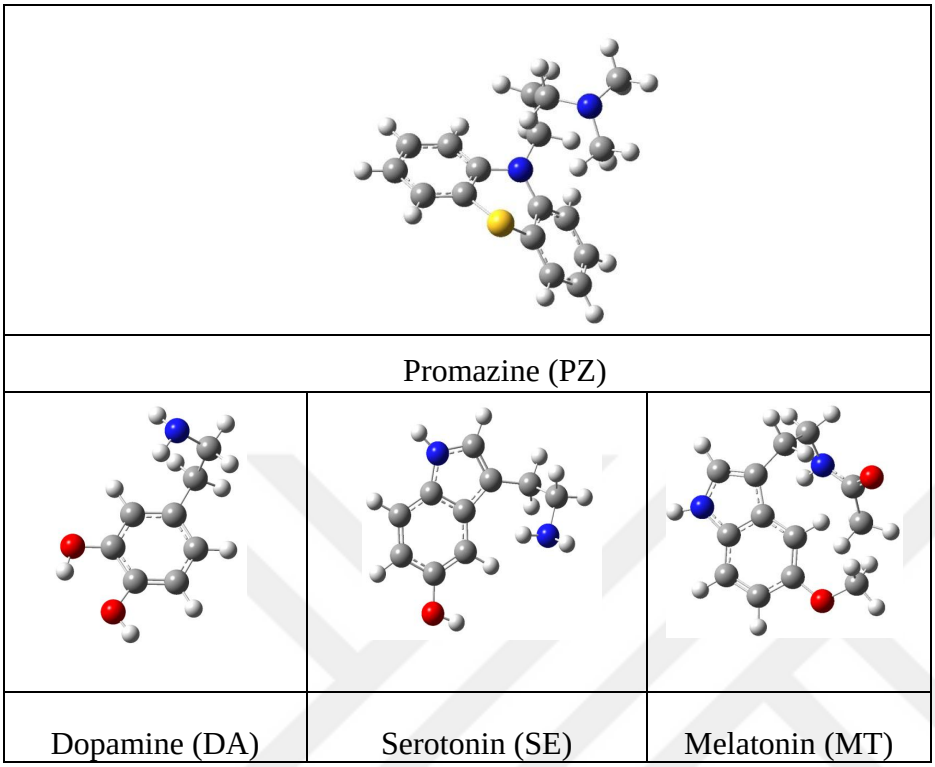

Figure 3.2. Optimized structures of the monomers of studied compounds

The properties of the used donor and acceptor systems are as follows: Promazine (98%, Sigma), Melatonin (98%, Sigma-Aldrich), Serotonin HCl (98%, Sigma-Aldrich), Dopamine HCl (Analytical, Fluka). Distilled water is used as solvent.

Sample solutions were treated to remove by bubbling through nitrogen for an extended period of time. The excitation wavelengths are chosen from UV-Vis absorption for all donor-acceptor complexes.

3.1.4 Computational methods

Theoretical calculations were performed with Gaussian09, Gaussview 5.0 and Spartan 08 to investigate various physical properties of the molecules (Frisch et al, 1998).

Specifically, DFT method used for this investigation. With the optimized geometries density functional theory (DFT) calculations were performed to

examine and compare the energies and band gaps of molecules. For the DFT calculations the ωB97XD functional was chosen with the 6-31G** basis set.

The excitation energies of molecules were calculated by the TD-DFT method, and the effects of electron donor and electron acceptor groups on the excitation energy as well as the orbital energies of HOMO and LUMO were examined.

Most studies of the fluorescence and absorption spectra and other photo physical properties of aromatic molecules are made in solution. The emitting or absorbing molecule is thus exposed to the influence of the surrounding molecules of the solvent, which can produce significant changes in its photophysical properties. The observed spectral and photophysical parameters are characteristic of the molecule in its solvent environment rather than of the isolated molecule (Lakowicz, 1999).

These compounds used in the study are as given in figure 3.3:

Acceptors:

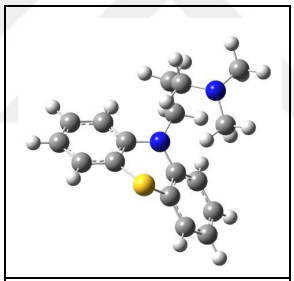

Promazine (PZ)

Donors:

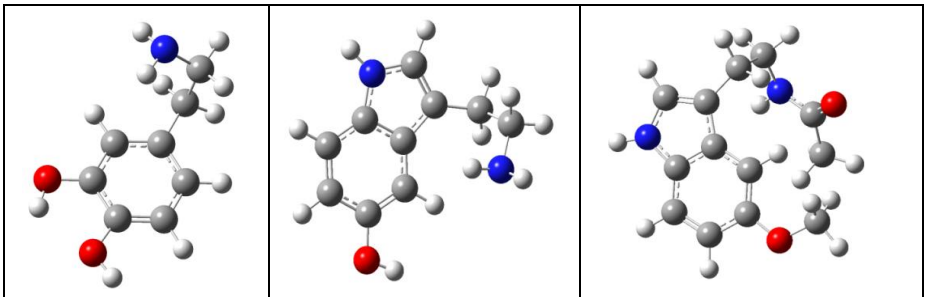

Dopamine (DA)	Serotonin (SE)	Melatonin (MT)

Figure 3.3. Molecular structure of donor and acceptor molecules.

4. RESULTS AND DISCUSSION

4.1. Computational Investigations

4.1.1 Geometry optimization

The geometries have been obtained by using Gaussian09 (Frisch et al.,2009), Gaussview5 (Gaussview 2005) and Spartan08 (Wavefunction, 2008) molecular modelling softwares. Ground state geometry optimizations are first performed at the ωB97XD/6-31G(d,p) level of DFT theory without symmetry constraint.

Optimized bond lengths between the carbon atoms in the electronic ground state have been obtained at DFT (Figure 4.1). Electronic energies, dipole moments, zero point energies and relative energies of promazine and hormones(dopamine, serotonin and melatonin) in vacum and in water are given in Tables 4.1 and 4.2. Table 4.3 shows calculated solvation free energies of studied promazine and hormones.

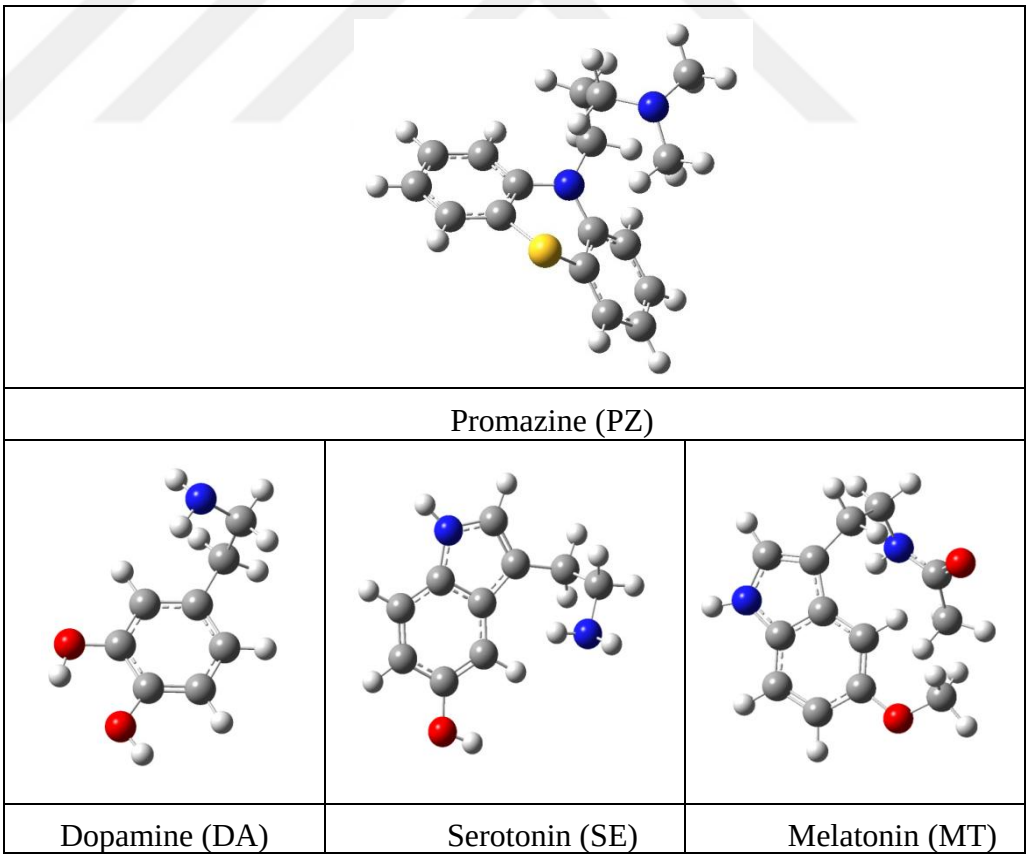

Figure 4.1. Optimized structures of the monomers of studied compounds

Table 4.1. Calculated total electronic energies (E_{elec}), dipole moments (μ), zero-point energy corrections (ZPE), lowest frequencies (Freq), complexation energies (ΔE) and free energy differences (ΔΔG) of studied compounds and their complexes in gas phase.

GAS	μ	E_{elec}	ZPE	E_{elec} + ZPE	E_{elec}+ΔG	Freq	ΔE	ΔΔG
	(D)	(Hartree)	(Hartree)	(Hartree)	(Hartree)	(cm^{-1})	(kcal/mol)	(kcal/mol)
PZ	2.36	-1167.302	0.341	-1166.961	-1167.006	33.74	-	-
DA	2.96	-516.521	0.185	-516.332	-516.372	51.92	-	-
SE	3.03	-572.852	0.211	-572.642	-572.677	71.39	-	-
MT	4.55	-764.773	0.279	-764.491	-764.537	41.27	-	-
PZ-DA	1.08	-1683.853	0.530	-1683.322	-1683.382	24.83	-18.20	-2.51
PZ-SE	2.02	-1740.181	0.556	-1739.623	-1739.686	15.49	-12.25	-1.88
PZ-MT	7.92	-1932.105	0.623	-1931.482	-1931.548	16.03	-18.83	-3.13

Table 4.2. Calculated total electronic energies (E_{elec}), dipole moments (μ), zero-point energy corrections (ZPE), lowest frequencies (Freq), complexation energies (ΔE) and free enegy differences (ΔΔG) of studied compounds and their complexes in water.

WATER	μ	E_{elec}	ZPE	E_{elec} + ZPE	E_{elec}+ΔG	Freq	ΔE	ΔΔG
	(D)	(Hartree)	(Hartree)	(Hartree)	(Hartree)	(cm^{-1})	(kcal/mol)	(kcal/mol)
PZ	3.65	-1167.310	0.342	-1166.96	-1167.01	35.95	-	-
DA	3.67	-516.533	0.185	-516.34	-516.382	49.91	-	-
SE	4.15	-572.865	0.211	-572.65	-572.691	62.40	-	-
MT	6.50	-764.788	0.278	-764.50	-764.55	41.34	-	-
PZ-DA	5.13	-1683.866	0.529	-1683.33	-1683.39	27.58	-18.83	-1.25
PZ-SE	3.08	-1740.200	0.555	-1739.64	-1739.706	18.95	-18.83	-3.77
PZ-MT	11.18	-1932.123	0.622	-1931.50	-1931.569	17.69	-25.10	-5.65

Table 4.3. Calculated solvation energies (E_{SOLV}) of studied promazine and hormones(dopamine, serotonin and melatonin).

Molecules	μ_v (D)	μ_s (D)	$E_{SOLV} = (E+ZPE)_S - (E+ZPE)_v$ (kcal/mol)
PZ	2.36	3.65	-4.89
DA	2.96	3.67	-7.53
SE	3.03	4.15	-8.22
MT	4.55	6.50	-9.41
PZ-DA	5.17	6.69	-8.67
PZ-SE	4.99	6.09	-12.16
PZ-MT	3.92	5.60	-12.14

Table 4.3 summarizes the solvation free energies for the studied systems. Free energy changes are not significant for molecules with small dipole moments in studided solvents.

The results indicate that promazine-melatonin (PZ-MT) complex is the most stable one in both media. However, the energy difference decreases in water. Free energy differences ($\Delta\Delta G$) indicate that promazine-serotonin (PZ-SE) complex forms easier in gas phase (Table 4.1) but promazine-melatonin (PZ-MT) complex forms easier in water (Table 4.2).

4.1.2 Electronic transitions

Electronic structures (molecular orbitals and their energies) of electron donor and acceptor molecules have been calculated at ωB97XD/6-31G** level with Density Functional Theory (DFT). The energy of highest occupied molecular orbital (HOMO) and lowest unoccupied molecular orbital (LUMO) transitions are shown for the molecules in gas phase and in water. Electron density plots for the HOMO and the LUMO orbitals at the ground state and excited state equilibrium geometry of the compounds are shown for the complexes.

4.1.2.1 Promazine (PZ)

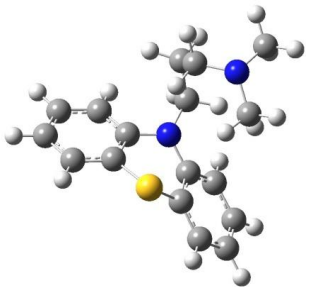

Figure 4.2. Optimized structure of promazine

Tables 4.4 and 4.5 display the electronic transitions (λ_{ex}), corresponding energy differences (ΔE), transition dipole moments ($\Delta\mu$), oscillator strengths (f), molecular orbitals and their % contributions of promazine (PZ) in gas phase and in water.

The main S_0-S_1 transitions in both media occur from HOMO to LUMO (Table 4.4 and Table 4.5). The oscillator strengths are very small for lower transitions but they significantly increase at higher transitions. The differences are more drastic in gas phase.

Table 4.4. Excited state properties predicted by quantum chemical model calculations for promazine in gas phase.

PZ GAS	ΔE (eV)	λ (nm)	Δμ (D)	f	Predominant Transitions	%
S1	4.379	283.13	0.0038	0.0004	H-1 → L H → L	19 65
S2	4.730	262.15	0.2025	0.0235	H-4→ L H-3→ L+2 H -2→ L+3 H-1 →L+1 H →L+4	16 13 15 17 62
S3	4.841	256.13	0.6850	0.0812	H-4→ L+3 H-3→ L+1 H-2→ L H-1→ L+2	13 17 24 18

					H →L +2	60
S4	5.437	228.04	0.6250	0.0833	H-2→ L	17
					H-2→ L+1	19
					H-1→ L+3	15
					H →L+2	11
					H →L+3	57
					H→ L+4	15
S5	5.437	226.63	1.4655	0.1964	H-5→L+4	10
					H-2→ L	37
					H-2→ L+4	19
					H-1→ L+4	13
					H →L+2	17
					H→L+3	26
					H→ L+4	38
S6	5.923	226.63	1.9337	0.2806	H-4→ L+3	10
					H-3→L+1	12
					H-2→ L	40
					H-2→L+4	13
					H-1→ L+4	13
					H →L+2	21
					H →L+4	43

Table 4.5. Excited state properties predicted by quantum chemical model calculations for promazine in water

PZ H_2O	ΔE (eV)	λ (nm)	Δμ (D)	f	Predominant Transitions	%
S1	4.368	283.91	0.0230	0.0025	H -1→ L	14
					H→L	66
S2	4.722	262.67	0.2990	0.0346	H-4→ L	15
					H-3→ L+2	13
					H -2→ L+3	14
					H-1→L+1	13
					H →L+1	64
S3	4.844	255.94	0.9972	0.1184	H-4→ L+3	12

					H-3→ L+1 H-2 →L H-1→L+2 H →L +2	17 22 13 61
S4	5.431	228.31	1.9962	0.2656	H-5 → L+4 H-2 → L H-2 → L+4 H →L+2 H → L+3 H → L+4	10 41 18 19 24 36
S5	5.460	227.07	0.9935	0.1329	H-2→ L H-2 → L+1 H-1 → L+3 H →L+3 H→L+4	16 18 10 59 17
S6	5.904	209.99	2.3489	0.3398	H-4→ L+3 H-3→ L H-3→ L+4 H-1→ L+4 H→L+2 H→ L+4	11 40 15 10 19 46

4.1.2.2 Dopamine (DA)

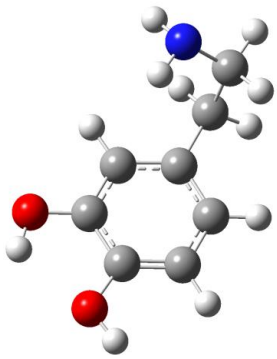

Figure 4.3. Optimized structure of dopamine

Table 4.6. Excited state properties predicted by quantum chemical model calculations for dopamine in gas phase

DA GAS	ΔE (eV)	λ (nm)	Δμ (D)	f	Predominant Transitions	%
S1	5.173	239.68	0.4741	0.0601	H-2→ L+1 H→L	31 62
S2	5.962	207.97	0.3912	0.0571	H-2→ L H-1→ L H→L+1	32 12 61
S3	6.847	181.09	2.5356	0.4253	H-2→ L H-2→ L+1 H-1→L H-1→L+1 H →L H→ L+1	50 18 12 30 18 26
S4	6.922	179.11	1.1390	0.1932	H-2→ L H-2→L+1 H-1→ L H-1→L+1 H→L H→L+1 H→ L+2	24 19 52 18 18 22 10
S5	6.931	178.88	0.0962	0.0163	H-2→ L H-2→L+2 H-1→L+2 H→L+2	12 13 11 64
S6	7.102	174.58	2.0388	0.3547	H-2→ L H-2→L+1 H-1→L H →L+1 H→ L	23 40 42 25 17

Tables 4.6 and 4.7 displays the electronic transitions (λ_{ex}), corresponding energy differences (ΔE), transition dipole moments (Δμ), oscillator strengths (f),

molecular orbitals and their % contributions of dopamine in gas phase and in water.

The main S_0-S_1 transitions in both media occur from HOMO to LUMO similar to promazine (Table 4.6 and Table 4.7). The oscillator strengths are very small for almost all transitions in contrast to the observed values for promazine.

Table 4.7. Excited state properties predicted by quantum chemical model calculations for dopamine in water.

DA H_2O	ΔE (eV)	λ (nm)	Δμ (D)	f	Predominant Transitions	%
S1	5.158	240.37	0.5891	0.0744	H-1→ L+1 H →L	31 63
S2	5.931	209.04	0.5771	0.0839	H-1 → L H→ L+1	32 62
S3	6.790	182.61	3.3825	0.5626	H-1→L H-1→L+1 H→L+1	60 16 31
S4	6.907	179.50	3.9148	0.6625	H -2→ L H-1→L H-1 → L+1 H→L	10 17 59 30
S5	7.239	171.28	0.2157	0.0383	H-2→L H-2→ L+1 H-1→ L+1	64 20 14
S6	7.280	170.31	0.0214	0.0038	H-2 → L H-2→L+1 H→L+4	11 66 11

4.1.2.3. Serotonin (SE)

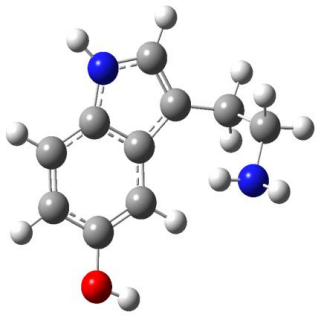

Figure 4.4. Optimized structure of serotonin

Tables 4.8 and 4.9 display the corresponding electronic transitions (λ_{ex}) for serotonin (SE) in gas phase and in water respectively. The main S_0-S_1 transitions in both media occur from HOMO to LUMO similar to promazine and dopamine (Table 4.8 and Table 4.9). The oscillator strengths are very small for almost all transitions like in dopamine but in contrast to promazine values.

Table 4.8. Excited state properties predicted by quantum chemical model calculations for serotonin in gas phase.

SE GAS	ΔE (eV)	λ (nm)	Δμ (D)	f	Predominant Transitions	%
S1	4.787	259.00	0.722	0.084	H-1→L H-1→ L+1 H→ L H→L+1	25 18 62 10
S2	5.198	238.54	0.821	0.104	H-1→ L H→ L H→ L-1	59 28 25
S3	6.537	189.66	3.665	0.587	H-3→ L H-1→L H→L+1	16 25 63
S4	6.642	186.66	0.904	0.147	H-3→L H-2→ L	21 14

					H-1→ L+1 H→ L	63 15
S5	6.906	179.54	0.244	0.041	H-2→ L H-1→L+1 H→ L+2	65 15 14
S6	7.087	174.95	1.127	0.195	H-3→ L H-2→ L H-1→ L H→L+2	39 18 11 51

Table 4.9. Excited state properties predicted by quantum chemical model calculations for serotonin in water.

SE H2O	ΔE (eV)	λ (nm)	Δμ (D)	f	Predominant Transitions	%
S1	4.760	260.45	0.8389	0.0978	H-1→L H-1→ L+1 H→L H→ L+1	29 16 61 11
S2	5.094	243.38	1.1311	0.1412	H-1→ L H→ L H→L+1	58 32 23
S3	6.396	193.85	5.1113	0.8009	H-1→ L H→L+1	26 64
S4	6.574	188.59	0.7761	0.1250	H-3→ L H-2→ L H-1→L+1 H→L	21 10 64 17
S5	6.9086	179.46	0.2883	0.0488	H-3→ L H-2→ L H-1→L+1 H→L+2	17 64 13 17
S6	7.080	175.11	0.7984	0.1385	H-3→ L H-2→L H→L+2	47 26 42

4.1.2.4. Melatonin (MT)

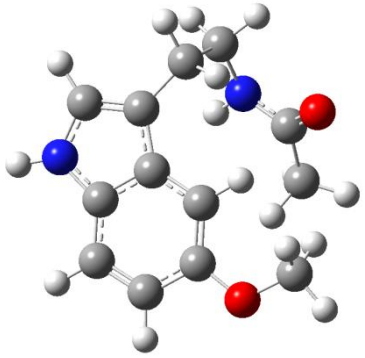

Figure 4.5. Optimized structure of melatonin

Tables 4.10 and 4.11 display the corresponding electronic transitions (λ_{ex}) for melatonin (MT) in gas phase and in water, respectively. The main S_0-S_1 transitions in both media occur from HOMO to LUMO similar to promazine, dopamine and serotonin (Table 4.10 and Table 4.11). The oscillator strengths are very small for almost all transitions like in dopamine and serotonin but in contrast to promazine values.

Table 4.10. Excited state properties predicted by quantum chemical model calculations for melatonin in gas phase.

MT GAS	ΔE (eV)	λ (nm)	Δμ (D)	f	Predominant Transitions	%
S1	4.796	258.52	0.6736	0.0791	H-1→L H-1→L+1 H-1→L+2 H→L	19 13 15 63
S2	5.210	237.95	0.8130	0.1038	H-1→ L H→L H→L+1 H→ L+2	62 22 17 17
S3	5.707	217.27	0.0210	0.0029	H-3→L+1 H-3→L+2 H-2→L+1 H-2→L+2	28 21 48 34

S4	6.432	192.75	3.2387	0.5104	H-4→ L H-1→ L H →L+1 H→L+2	13 23 54 34
S5	6.575	188.58	1.1433	0.1842	H-4 →L H-1→L+1 H-1 → L+1 H → L+2 H → L+1	12 52 38 18 11
S6	6.868	180.52	0.4719	0.0794	H-3→ L+1 H-1 → L+2 H→ L+1 H→ L+2 H →L+3	12 22 34 52 11

Table 4.11 Excited state properties predicted by quantum chemical model calculations for melatonin in water.

MT H_2O	ΔE (eV)	λ (nm)	Δμ (D)	f	Predominant Transitions	%
S1	4.787	258.90	0.7787	0.0913	H-1→ L H-1→ L+2 H→L	31 14 60
S2	5.093	243.40	1.1508	0.1436	H -1→ L H → L H→ L+1 H→ L+2	57 34 13 17
S3	5.852	211.85	0.0217	0.0031	H-3 → L+1 H-3 → L+2 H-2 → L+1 H-2 →L+2	41 27 41 26
S4	6.340	195.55	4.6544	0.7230	H-1 → L H →L+1 H → L+2	24 50 42
S5	6.487	191.13	1.0942	0.1739	H-4 →L	14

					H-1 →L+1 H-1 →L+1 H →L	48 44 15
S6	6.792	182.54	0.2454	0.0408	H-3→ L+1 H-1→ L+2 H →L+1 H →L+2	12 13 44 50

The frontier molecular orbitals (MOs) of electronically excited states of studied molecules are displayed in Figure 4.6. Both HOMO and LUMO are located mostly on the rings for all studied monomers. This observation is valid for orbitals both in gas phase and in water. The results displayed for promazine and the hormones (Dopamine, Serotonin and Melatonin) indicate that there are no significant changes in the properties and molecular orbitals in gas phase and in water. Also, electron transition is easier in water than in gas phase.

	GAS PHASE			WATER		
	HOMO	**LUMO**	**ΔE**	**HOMO**	**LUMO**	**ΔE**
Promazine	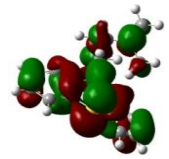	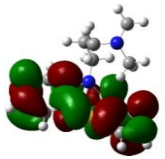	4.379 eV	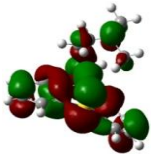	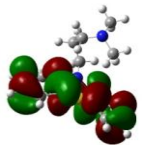	4.367 eV
Dopamine	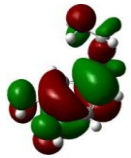	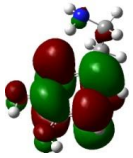	5.172 eV	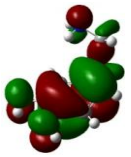	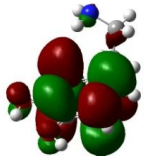	5.158 eV
Serotonin	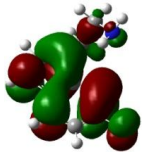	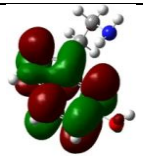	4.787 eV	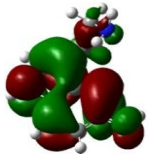	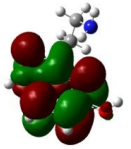	4.760 eV
Melatonin	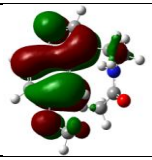	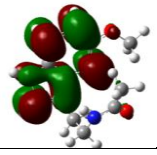	4.796 eV	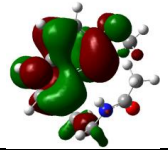	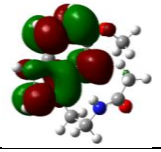	4.787 eV

Figure 4.6. Frontier molecular orbitals of studied molecules involved in the CI-description of lowest excited singlet states (in gas phase and in water)

4.1.3 Promazine and hormones (Dopamine, Serotonin and Melatonin) systems

4.1.3.1 Promazine-Dopamine (PZ-DA)

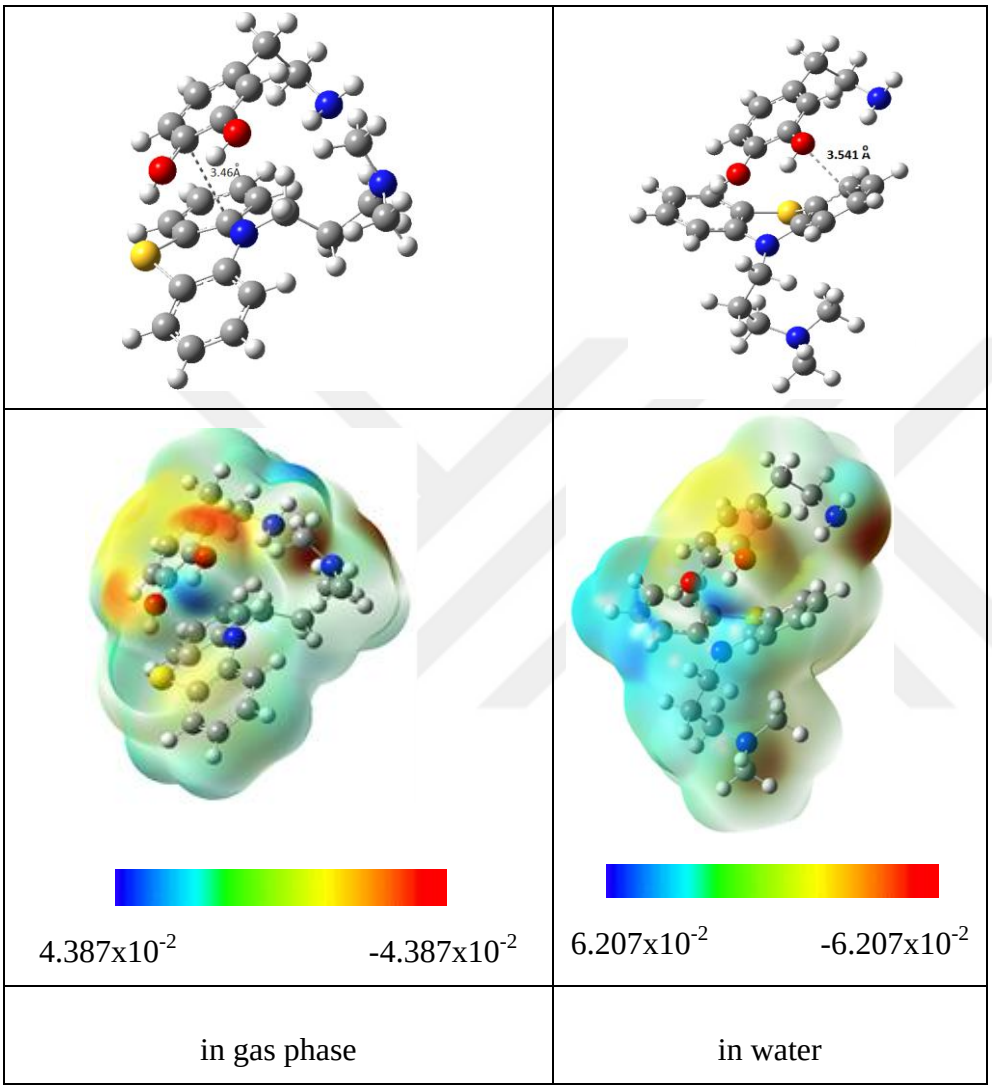

Figure 4.7. Optimized structures of promazine- dopamine complexes in gas phase and in water

Promazine-dopamine complexes have different geometries in gas phase and in water (Figure 4.7). The aromatic ring of dopamine is always oriented towards the isoalloxazine ring of promazine but the orientation of the $–NH_2$ terminal group changes in water as it is directed towards the ring part of promazine rather than the $–N(CH_3)_2$ group as in gas phase.

When electronic excitations are examined in gas phase (Table 4.12), it is oberved that the $S_0 \rightarrow S_1$ transition is a local excitation of promazine (LE1) (Figure 4.8). The first charge transfer from promazine to dopamine (CT1) is observed at $S_0 \rightarrow S_3$ from H-4 and H-3 to L. However, its magnitude is low and the main process is LE1. At $S_0 \rightarrow S_4$, both charge transfer from promazine to dopamine (CT1) and charge transfer from dopamine to promazine (CT2) are observed. Although, there are slight local excitations (LE1) observed, the main processes are CT1 and CT2, former predominating. Both $S_0 \rightarrow S_5$ and $S_0 \rightarrow S_6$ transitions have mainly charge transfer character. It is clearly seen that charge transfer increases significantly at higher transitions in gas phase.

Table 4.12. Excited state properties predicted by quantum chemical model calculations for promazine- dopamine system in gas phase

PZ-DA	ΔE (eV)	λ (nm)	Δμ (D)	f	Character	Predominant Transitions	%
S1	4.045	306.50	0.1404	0.0139	LE1	H→L	68
S2	4.624	268.12	0.2176	0.0247	LE1	H → L+1	65
S3	4.729	262.16	0.6113	0.0708	CT1+LE1	H-4 →L	12
					CT1+LE1	H-3 →L	22
					LE1	H →L+2	61
S4	5.099	243.18	0.2101	0.0262	LE1+CT1	H-4 →L+4	22
					CT1+LE1	H-3 →L+4	15
					CT1+CT2	H-2 →L+3	19
					CT2	H-1→L+3	56
S5	5.352	231.64	1.8340	0.2405	CT2+LE1	H-4 →L	15
					CT2+LE1	H-3 →L	29
					CT2+LE1	H-1→L	18
					LE1	H →L	11
					LE1	H →L+2	20
S6	5.568	222.65	0.3324	0.0454	CT2+LE1	H-3 →L+1	17
					CT2	H-1 →L	14
					CT2	H-1 →L+1	11
					LE1+CT1	H →L+3	50
					LE1+CT1	H →L+4	18

LE1: locally excited promazine, LE2: locally excited dopamine, CT1: charge transfer from promazine to dopamine, CT2: charge transfer from dopamine to promazine

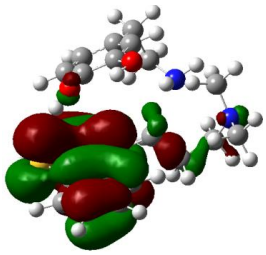	HOMO -7.07 eV	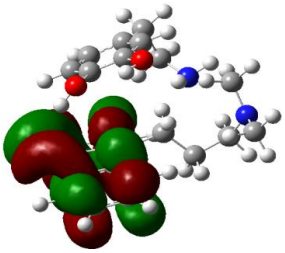	LUMO 1.17 eV
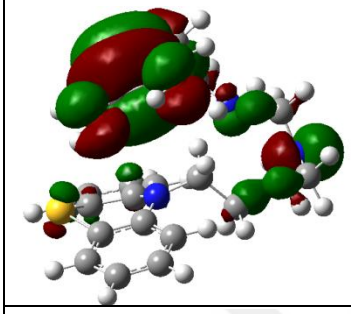	H – 1 -7.43 eV	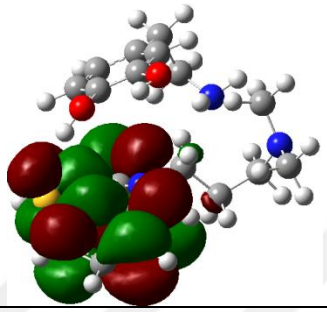	L + 1 1.50 eV
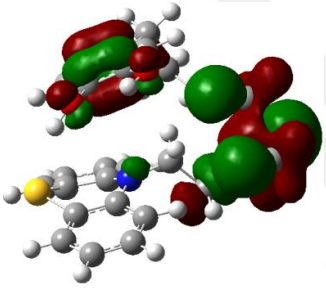	H – 2 -7.73 eV	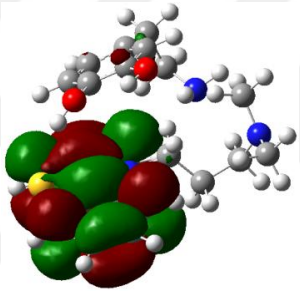	L + 2 1.69 eV
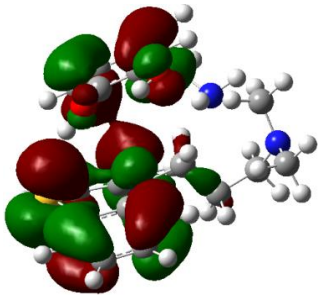	H – 3 -8.52 eV	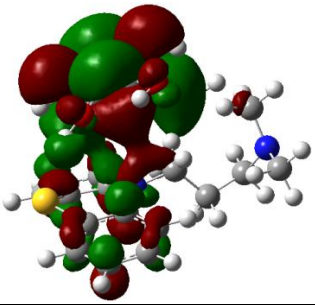	L + 3 2.00 eV
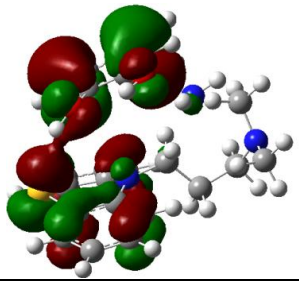	H – 4 -8.54 eV	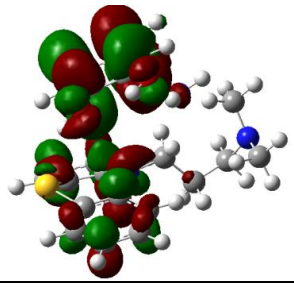	L + 4 2.39 eV

Figure 4.8. Frontier molecular orbitals of promazine-dopamine system in gas phase involved in the CI-description of lowest excited singlet states

Table 4.13 and Figure 4.9 display the molecular orbitals and excited properties of promazine-dopamine system calculated in water. In contrast to gas phase, the $S_0 \rightarrow S_1$ transition corresponds to charge transfer from dopamine to promazine (CT2) accompanied by a locally excited promazine (LE1) (Table 4.13). H→L+1 transition is the most abundant one (51%). In all other transitions except $S_0 \rightarrow S_3$ charge transfer is the main process, but $S_0 \rightarrow S_3$ transition has been mostly dominated by locally excited promazine (LE1) and dopamine (LE2).

Table 4.13. Excited state properties predicted by quantum chemical model calculations for promazine-dopamine system in water.

PZ-DA	ΔE (eV)	λ (nm)	Δμ (D)	f	Character	Predominant Transitions	%
S1	4.332	286.19	0.0245	0.0026	LE1+CT2	H-2→ L	11
					LE1+CT2	H-2→L+1	13
					LE1	H→L	42
					LE1+CT2	H →L+1	51
S2	4.593	269.93	0.4854	0.0546	LE1+CT2	H-2 →L	14
					LE1+CT2	H →L	49
					LE1+CT2	H → L+1	41
S3	4.759	260.52	0.6973	0.0813	LE1+CT2	H-3→ L+1	14
					LE1+LE2	H-2→ L+2	13
					LE1+LE2	H →L+2	62
S4	5.136	241.43	0.3529	0.0444	LE1+CT2	H-2→L+2	10
					LE1+CT1	H-2 → L+4	19
					LE1+CT2	H-1 → L+2	21
					LE1+CT2	H-1 → L+3	21
					LE1+CT2	H-1→ L+4	46
					CT2+LE1	H→ L+4	16
S5	5.395	229.80	1.1683	0.1544	CT2	H-3 → L	16
					CT2	H-3 → L+1	36
					LE1+LE2	H →L+2	16
					LE1+CT2	H→ L+3	25
					LE1+CT2	H→L+4	12
S6	5.440	227.92	0.8609	0.1147	CT1	H-3 → L	23
					LE1+CT1	H-2→ L+3	11

					LE1+CT1 LE1+CT1	H →L+3 H → L+4	54 17

LE1: locally excited promazine, LE2: locally excited dopamine, CT1: charge transfer from promazine to dopamine, CT2: charge transfer from dopamine to promazine

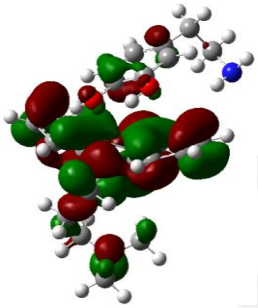	HOMO -7.18 eV	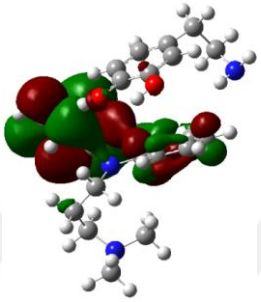	LUMO 1.25 eV
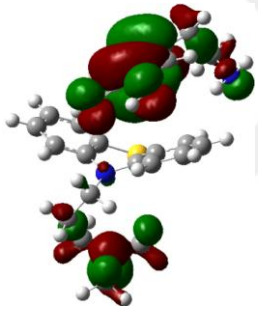	H – 1 -7.54 eV	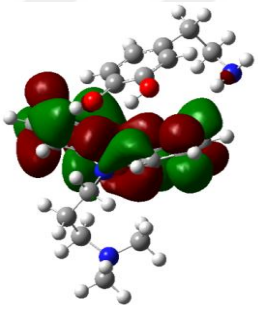	L + 1 1.31 eV
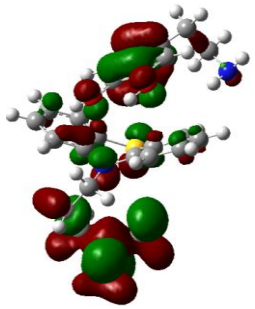	H – 2 -7.59 eV	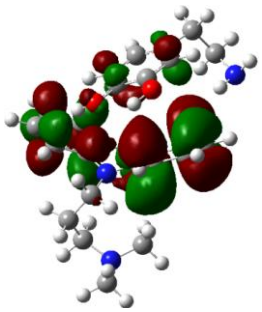	L+2 1.55 eV
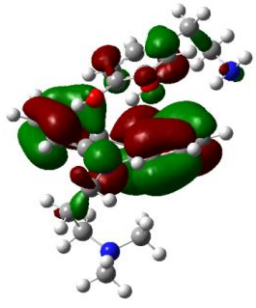	H – 3 -8.30 eV	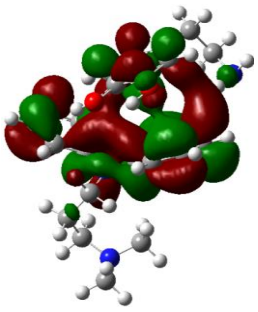	L + 3 1.96 eV

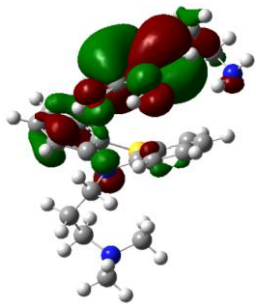	H – 4 -8.46 eV	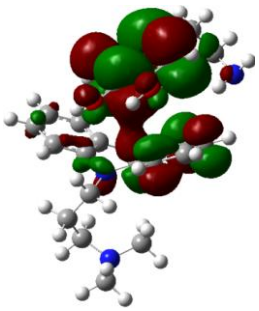	L+4 2.07 eV

Figure 4.9. Frontier molecular orbitals of promazine-dopamine system in water involved in the CI-description of lowest excited singlet states

4.1.3.2 Promazine-Serotonin (PZ-SE)

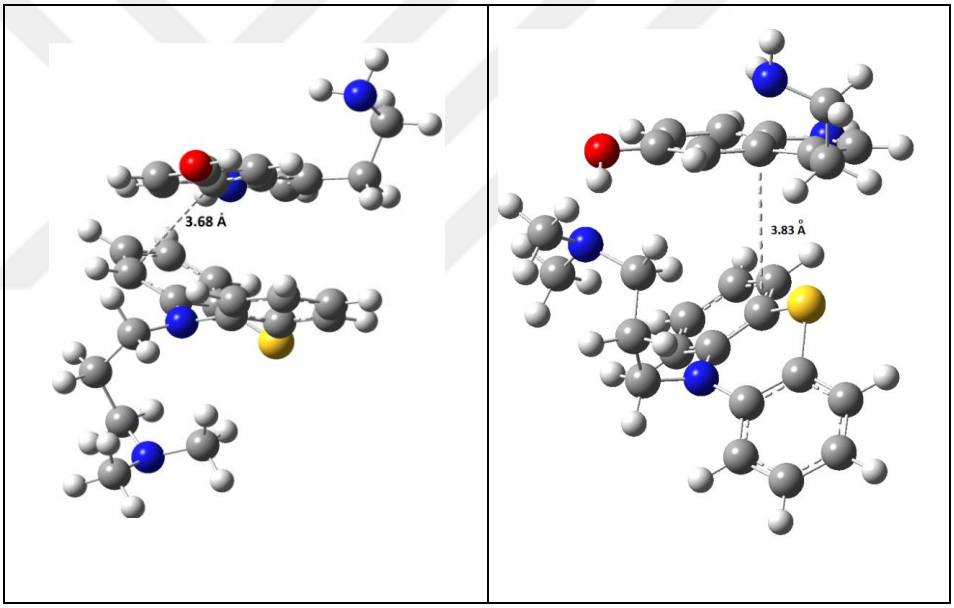

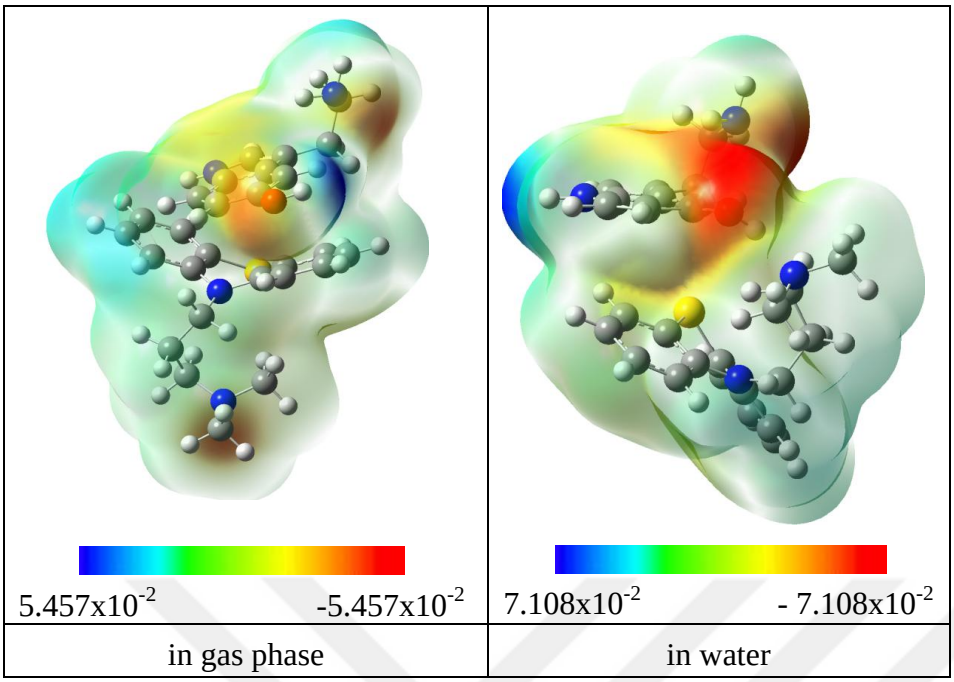

Figure 4.10. Optimized structures of promazine-serotonin complexes in gas phase and in water

Promazine-serotonin complexes have also different geometries in gas phase and in water (Figure 4.10). The aromatic rings of promazine and serotonin face each other in gas phase but the orientation of the –OH side chain on the phenyl ring of serotonin directed towards the $–N(CH_3)_2$ group in water. Slight distortion of the OH hydrogen may indicate presence of a hydrogen bonding.

When electronic excitations are examined in gas phase (Table 4.14), it is observed that the $S_0 \rightarrow S_1$ transition is a mixture of charge transfer from promazine to serotonin (CT1), charge transfer from serotonin to promazine (CT2), locally excited promazine (LE1), and locally excited serotonin (LE2) (Figure 4.11). The main contribution comes from H-1→L (55%) which corresponds to LE1+CT1. The results are similar for other higher transitions. It may be concluded that promazine-serotonin system has a tendency for charge transfer in gas phase in contrast to the promazine-dopamine system.

Table 4.14. Excited state properties predicted by quantum chemical model calculations for promazine-serotonin system in gas phase.

PZ-SE	ΔE (eV)	λ (nm)	Δμ (D)	f	Character	Predominant Transitions	%
S1	4.278	289.85	0.0223	0.0023	CT1+LE1	H-3→L	18
					LE1+CT1	H-1→ L	55
					CT2+LE1	H-1→ L+1	29
					CT2+LE2	H →L	14
S2	4.600	269.52	0.3134	0.0353	LE1	H-3 → L+1	17
					LE1+CT1	H-1→L	26
					CT2+LE1	H-1→L+1	53
					CT1+LE1	H-1→L+2	10
					CT2+LE2	H →L	11
					CT2	H→L+1	11
S3	4.685	264.65	0.4280	0.0491	CT2+LE2	H-2→ L+2	21
					CT2+LE2	H-2→ L+3	11
					LE1+CT1	H-1→L	13
					CT2+LE1	H-1→ L+1	10
					LE2+CT2	H →L	25
					LE2+CT2	H→ L+2	42
					LE2+CT2	H →L+3	30
					LE2+CT2	H→ L+4	10
S4	4.805	258.03	0.3350	0.0394	CT1+LE2	H-4→ L	13
					CT2	H-4 → L+1	10
					LE1+LE2	H-4 → L+4	14
					CT1+LE1	H-3 → L-2	11
					CT1+LE1	H-3 → L-3	12
					LE1+CT1	H-1 → L+2	41
					LE1+CT1	H-1 → L+3	40
					CT2+LE2	H → L+2	13
					CT2+LE2	H → L+3	13
S5	4.996	248.16	0.3271	0.0400	CT2+LE2	H-2→ L	27
					CT2+LE2	H-2→ L+2	43
					CT2+LE2	H-2→ L+3	27

					CT2+LE2	H→ L	19
					CT2+LE2	H→L+2	24
S6	5.315	233.28	0.6057	0.0789	LE2+CT1	H-4→ L+1	12
					CT1+LE1	H-1→ L	12
					CT2+LE1	H-1→L+1	14
					CT1+LE1	H-1→ L+2	18
					CT2+LE2	H →L	39
					CT2	H → L+1	34
					CT2+LE2	H → L+2	13
					CT2+LE2	H → L+3	12
					CT2+LE2	H → L+4	17

LE1: locally excited promazine, LE2: locally excited serotonin, CT1: charge transfer from promazine to serotonin, CT2: charge transfer from serotonin to promazine

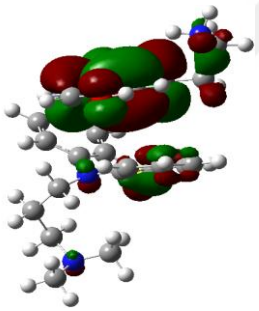	HOMO -6.97 eV	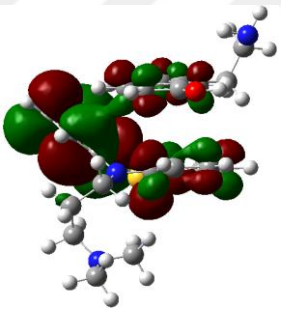	LUMO 1.31 eV
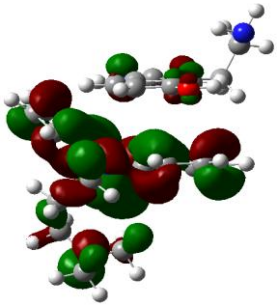	H – 1 -7.05 eV	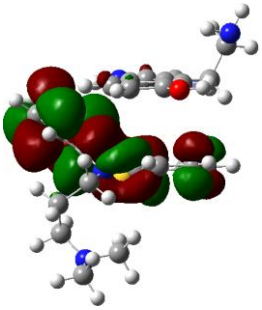	L + 1 1.50 eV

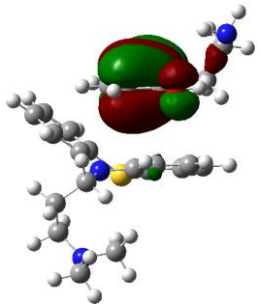	H – 2 -7.27 eV	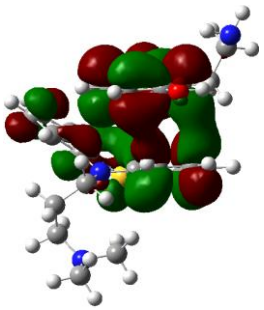	L + 2 1.69 eV
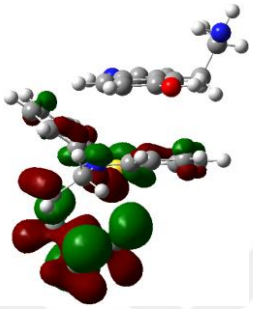	H – 3 -7.35 eV	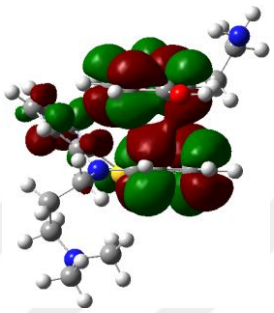	L + 3 1.90 eV
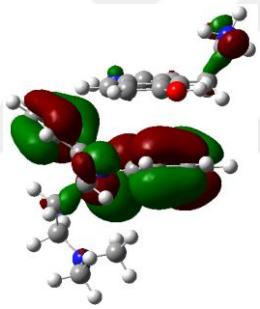	H – 4 -8.11 eV	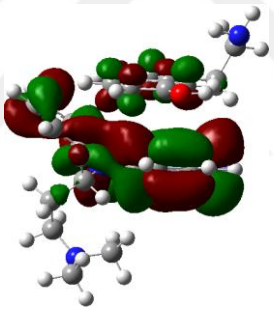	L + 4 2.23 eV

Figure 4.11. Molecular orbitals of promazine-serotonin system in gas phase involved in the CI-description of lowest excited singlet states

Table 4.15 and Figure 4.12 display the molecular orbitals and excited state properties of promazine-serotonin system calculated in water. In water, CT2 disappears for the $S_0 \rightarrow S_1$ transition and the main transition from H→L corresponds to a mixture of LE1+LE2 (64%) (Table 4.15). In other transitions CT and LE states are separated more significantly compared to gas phase. Results in water also indicate that promazine-serotonin system has more tendency for charge transfer compared to promazine-dopamine system.

Table 4.15. Excited state properties predicted by quantum chemical model calculations for promazine-serotonin system in water.

PZ-SE	ΔE (eV)	λ (nm)	Δμ (D)	f	Character	Predominant Transitions	%
S1	4.199	295.26	0.0608	0.0063	CT2	H-1→ L	17
					LE1+LE2	H→L	64
					CT1+LE1	H→ L+2	12
S2	4.592	269.96	0.2231	0.0251	LE1	H-3→L+4	12
					CT2	H-1→ L+1	13
					CT2+LE1	H-1→L+2	11
					LE1+LE2	H→L+1	61
					CT1	H→L+2	14
S3	4.688	264.45	0.5006	0.0575	CT2	H-2→ L+2	20
					CT2	H-1→ L	21
					CT2	H-1→L+1	17
					LE1+CT2	H-1→ L+2	50
					CT2	H-1→ L+3	18
					CT1	H→L+2	19
S4	4.738	261.65	1.0836	0.1258	LE1	H-3→ L	20
					LE1+CT2	H-1→ L+2	11
					CT2	H-1→ L+3	13
					CT1	H→L+2	21
					LE1+LE2	H→ L+3	57
S5	5.082	243.94	0.8411	0.1047	CT2	H-2 → L	19
					CT2	H-2→L+1	17
					CT2+LE2	H-2→ L+2	52
					CT2+LE2	H-2→ L+3	26
					CT1	H-1→ L+1	12
					LE1+CT2	H-1→ L+2	22
S6	5.324	232.88	0.6924	0.0903	CT2	H-3→ L+1	16
					CT2	H-1→ L+4	15
					CT1+LE1	H→L+2	15
					CT2	H→ L+4	62

LE1: locally excited promazine, LE2: locally excited serotonin, CT1: charge transfer from promazine to serotonin, CT2: charge transfer from serotonin to PZ

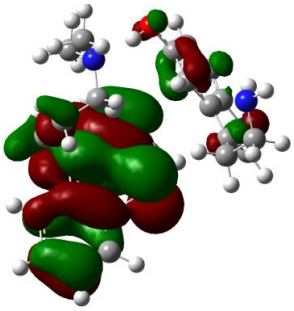	HOMO -7.05 eV	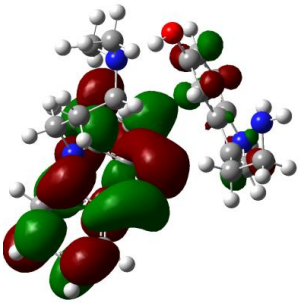	LUMO 1.33 eV
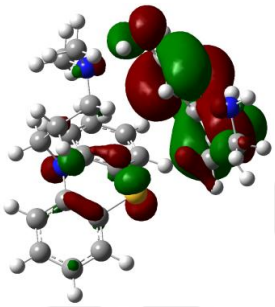	H – 1 -7.13 eV	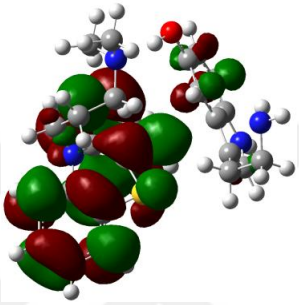	L + 1 1.52 eV
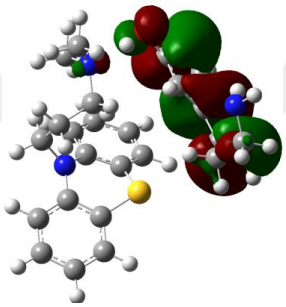	H – 2 -7.43 eV	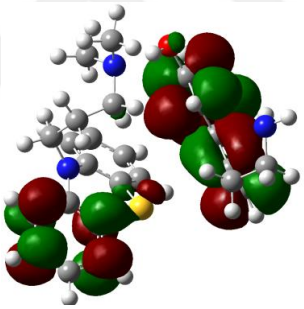	L + 2 1.61 eV
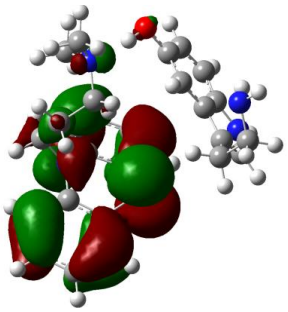	H – 3 -8.16 eV	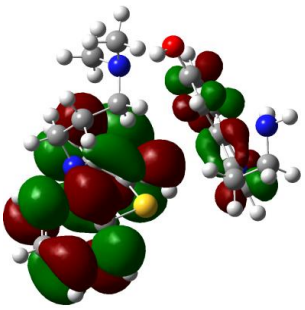	L + 3 1.74 eV

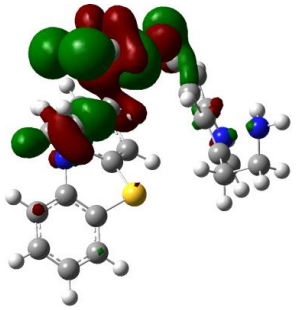	H – 4 -8.41 eV	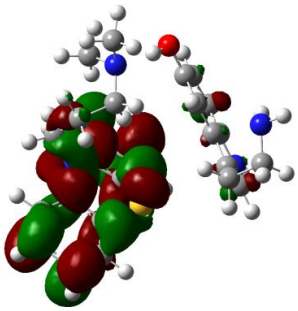	L + 4 2.10 eV

Figure 4.12. Molecular orbitals of promazine-serotonin system in water involved in the CI-description of lowest excited singlet states

4.1.3.3 Promazine-Melatonin (PZ-MT)

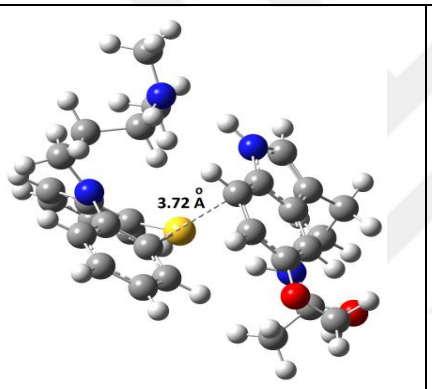	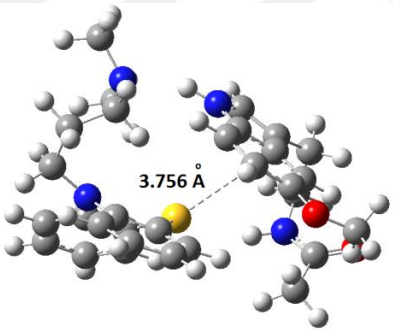
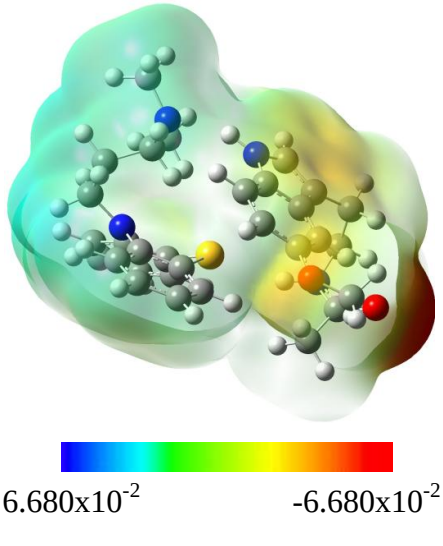	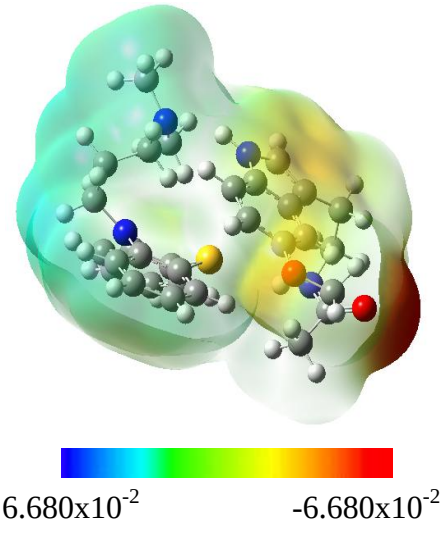
in gas phase	in water

Figure 4.13. Optimized structures of promazine-melatonin complexes in gas phase and in water

In contrast to former two systems, promazine-melatonin complexes have similar geometries in gas phase and in water (Figure 4.13). The aromatic rings of promazine and melatonin face each other both in gas phase and in water. Although these is a slight distortion in the complex geometry, the general structure remains same.

When electronic excitations are examined in gas phase (Table 4.16), it is observed that the $S_0 \rightarrow S_1$ transition is a mixture of charge transfer from melatonin to promazine (CT2), locally excited promazine (LE1), and locally excited melatonin (LE2) (Figure 4.14). The main contribution comes from H-2→L (62%) which corresponds to CT2+LE1. The results are similar for higher transitions, but charge transfer from promazine to melatonin (CT1) starts at $S_0 \rightarrow S_3$ transition. It may be concluded that promazine-melatonin system has a tendency for charge transfer in gas phase similar to promazine-serotonin system but in contrast to the promazine-dopamine system.

Table 4.16. Excited state properties predicted by quantum chemical model calculations for promazine-melatonin in gas phase

PZ-MT	ΔE (eV)	λ (nm)	Δμ (D)	f	Character	Predominant Transitions	%
S1	4.415	280.8	0.0029	0.0003	CT2+LE1	H-2 → L	62
					LE1+LE2	H-2 → L+1	16
					CT2	H-1 → L	19
S2	4.750	261.0	0.2879	0.0335	LE1+LE2	H-2 → L+1	32
					CT2+LE2	H-1 → L+3	21
					CT2+LE2	H-1 → L+4	16
					CT2	H → L+1	12
					CT2+LE2	H → L+3	40
					CT2+LE2	H → L+4	26
S3	4.760	260.5	0.5434	0.0634	CT2	H-2 → L	14
					LE1+LE2	H-2 → L+1	48
					CT1+LE1+LE2	H-2 → L+3	11
					CT1	H-1 → L+1	20
					CT1+LE1+LE2	H-1 → L+3	10
					CT1+LE1+LE2	H → L+3	24
					CT1+LE1+LE2	H → L+4	16

S4	4.883	253.9	0.4336	0.0519	LE1+CT2	H-3 → L	22
					LE1+CT2	H-3 → L+1	11
					LE1+CT2	H-2 → L+2	56
					CT2	H-1 → L+2	21
S5	5.048	245.6	0.4763	0.0589	CT2	H-1 → L+1	15
					CT2+LE1+LE2	H-1 → L+3	44
					CT2+LE1+LE2	H-1 → L+4	27
					CT1+LE1+LE2	H-2 → L+3	26
					CT1+LE1+LE2	H-2 → L+4	20
S6	5.428	228.4	1.0953	0.1457	LE1+CT1	H-3 → L	26
					CT1+LE1+LE2	H-2 → L+3	38
					CT1+LE1+LE2	H-2 → L+4	29
					CT2	H-1 → L	13
					CT2+LE2+LE1	H-1 → L+3	11
					CT2+LE2+LE1	H-1 → L+4	17

LE1: locally excited promazine, LE2: locally excited melatonin, CT1: charge transfer from promazine to melatonin, CT2: charge transfer from melatonin to promazine

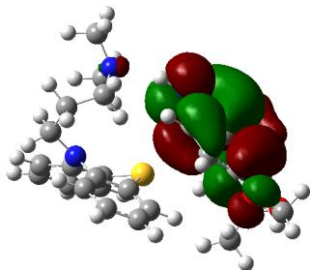	HOMO -6.86 eV	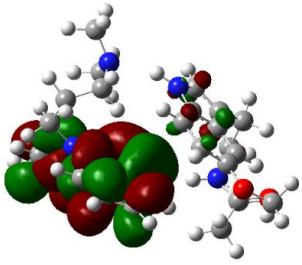	LUMO 1.36 eV
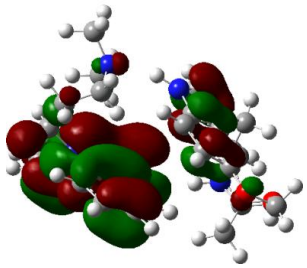	H – 1 -7.05 eV	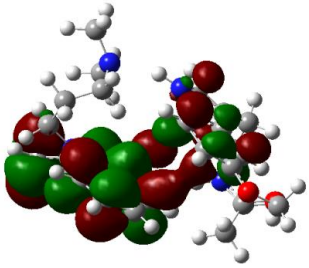	L + 1 1.47 eV

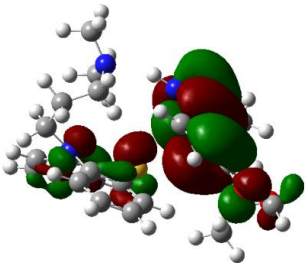	H – 2 -7.29 eV	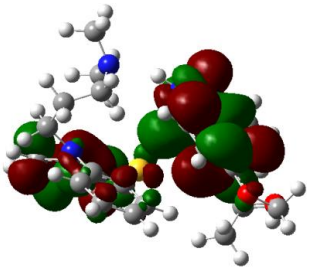	L + 2 1.71 eV
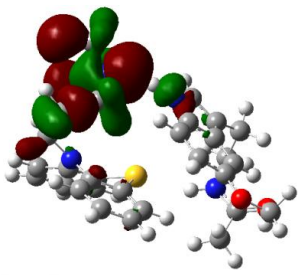	H – 3 -8.27 eV	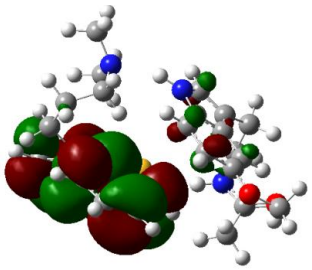	L + 3 1.90 eV
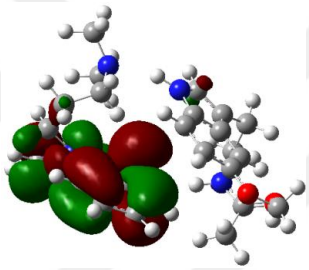	H – 4 -8.30 eV	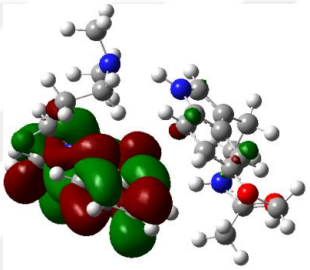	L + 4 2.04 eV

Figure 4.14. Molecular orbitals of promazine-melatonin system in gas phase involved in the CI-description of lowest excited singlet states

Table 4.17 and Figure 4.15 display the molecular orbitals and excited state properties of promazine-melatonin system calculated in water. In water, $S_0 \rightarrow S_1$ transition has CT2 characters. The main transition from H-1→L corresponds to CT2 (64%) (Table 4.17). On the other hand, higher transitions are mixtures of CT1, CT2, LE1 and LE2. Results in water also support the conclusion that promazine-melatonin system has a tendency for charge transfer similar to promazine-serotonin system which is in contrast to the promazine-dopamine system.

Table 4.17. Excited state properties predicted by quantum chemical model calculations for promazine-melatonin system in water.

PZ-MT	ΔE (eV)	λ (nm)	Δμ (D)	f	Character	Predominant Transitions	%
S1	4.379	283.16	0.0096	0.0010	CT2	H-2 → L	20

					CT2	H-1 → L	64
					CT1	H-1 → L+2	10
S2	4.738	261.72	0.2518	0.0292	LE1	H-4 → L+4	13
					CT2	H-2 → L+1	22
					LE1+LE2	H-1 → L+1	52
					CT1	H-1 → L+2	24
					CT2	H → L+2	18
S3	4.752	260.92	0.7409	0.0863	CT2+LE2	H-2 → L+2	29
					LE1+LE2	H-1 → L+1	26
					CT2	H → L	13
					CT2+LE2	H → L+1	23
					CT2+LE2	H → L+2	44
S4	4.866	254.83	0.7628	0.0909	LE1+CT1	H- 4→ L	23
					CT2+LE2	H-2 → L+3	17
					CT1+LE1	H-1 → L+2	13
					LE1+CT2	H-1 → L+3	57
S5	4.993	248.35	0.7907	0.0967	CT2+LE1	H-2 → L	13
					LE1+CT2	H-2 → L+1	23
					LE1+LE2	H-2 → L+2	42
					CT1+LE1	H-1 → L+2	17
					CT2+LE2	H → L+1	16
					LE2+CT2	H → L+2	32
S6	5.401	229.57	1.7002	0.2250	LE1+CT1	H-4 → L	33
					CT1+LE1	H-4 → L+1	12
					LE1+CT2	H-1 → L+3	20
					LE1+CT2	H-1 → L+4	33
					CT2	H-1 → L+5	14
					CT2	H-1→ L+6	26

LE1: locally excited promazine, LE2: locally excited melatonin, CT1: charge transfer from promazine to melatonin, CT2: charge transfer from melatonin to promazine

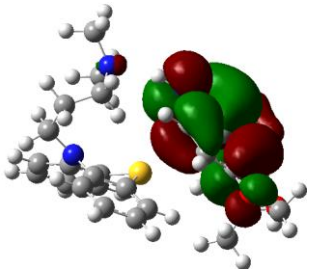	HOMO -7.13 eV	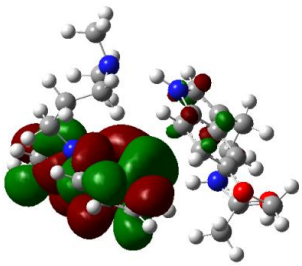	LUMO 1.36 eV
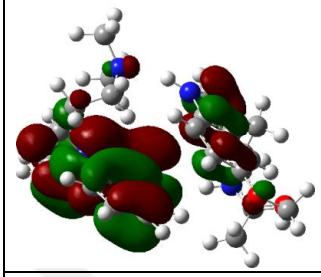	H – 1 -7.21 eV	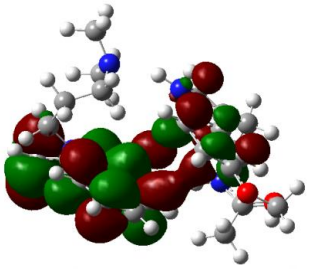	L + 1 1.47 eV
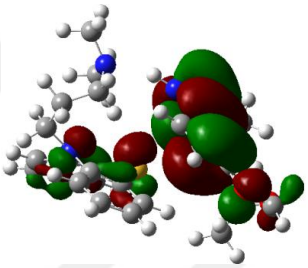	H – 2 -7.35 eV	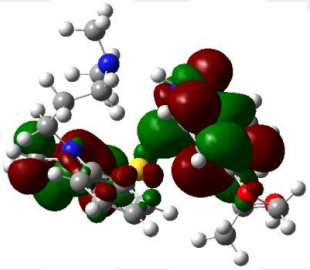	L + 2 1.66 eV
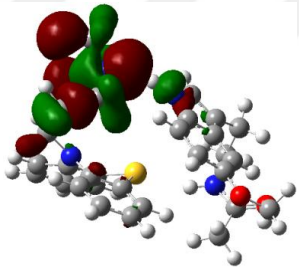	H – 3 -8.14 eV	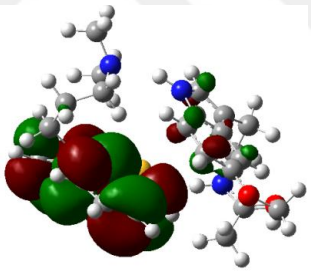	L + 3 1.71 eV
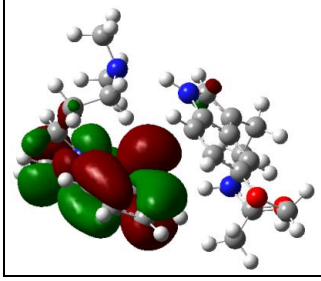	H – 4 -8.24 eV	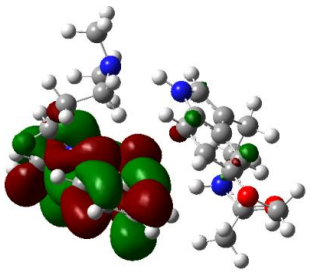	L + 4 2.01 eV

Figure 4.15. Molecular orbitals of promazine-melatonin system in water involved in the CI-description of lowest excited singlet states

4.2. Experimental Investigations

The following methods were used for the investigation of absorption and emission spectra. Preliminarily the donor and acceptor solutions were optimized

by recording the absorption and emission data at λ_{max} for a series of selected donor and acceptor solutions in varying concentrations.

4.2.1 Promazine (PZ)

Promazine has strong absorption intensity in water (Fig. 4.16). It shows two peaks in UV region at 302 and 252 nm. Promazine concentration was kept constant at $2.4x10^{-5}$ M in the study.

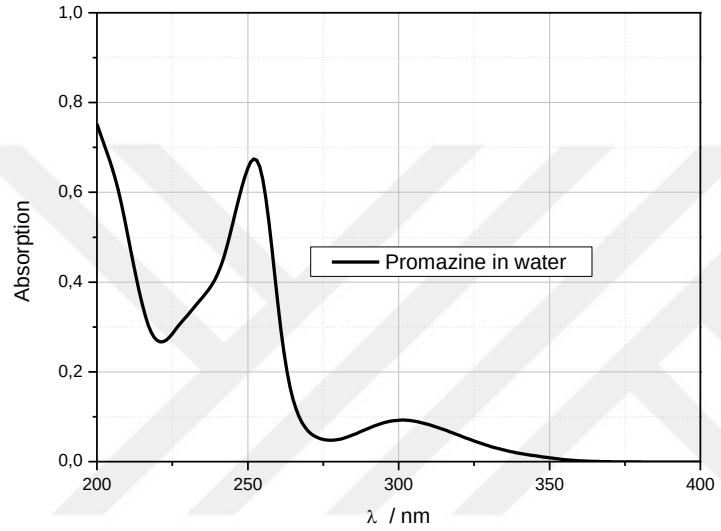

Figure 4.16. UV/Vis absorption spectrum of $2.24x10^{-5}$M promazine in water

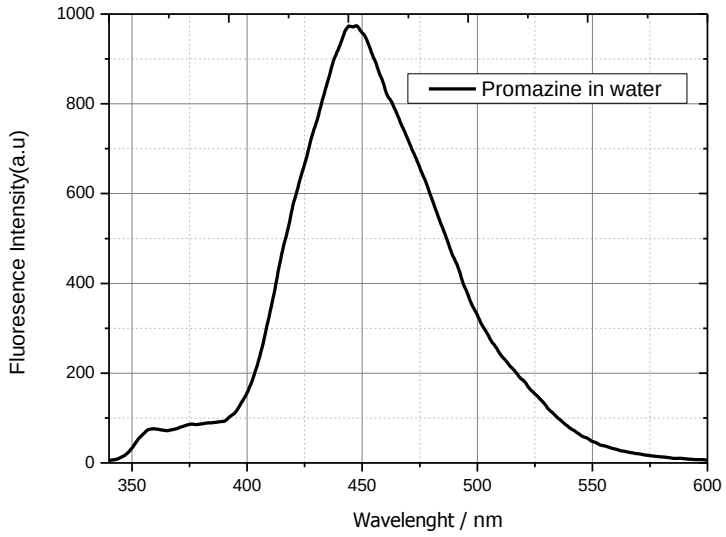

Figure 4.17. Fluorescence spectrum of $8.00x10^{-5}$M promazine in water λ_{ex}=330 nm.

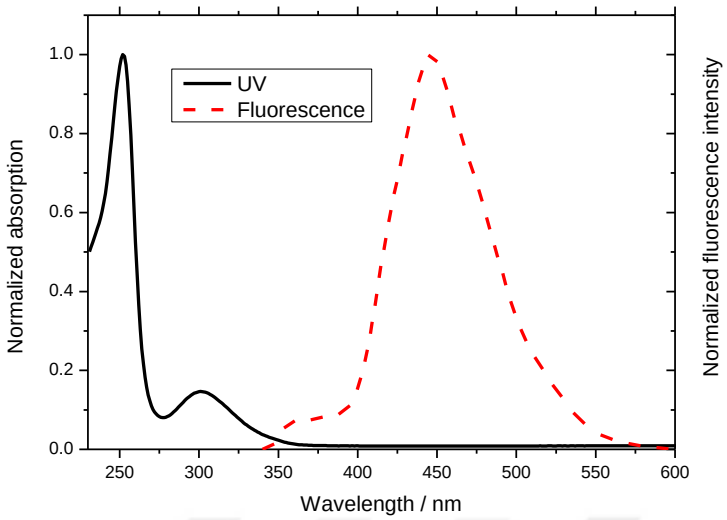

Figure 4.18. Normalized absorption and fluorescence spectrum of promazine in water.

Normalized Absorption and Fluorescence Spectra of Promazine in water was shown in Fig. 4.17. Wavelength was found from the spectra at 350 nm (Fig. 4.18).

4.2.2 Dopamine (DA)

Dopamine has also strong absorption spectrum in UV region. Figure 4.19 shows absorption spectrum of Dopamine at $1x10^{-4}$ M in water. It has a peak at 280 nm.

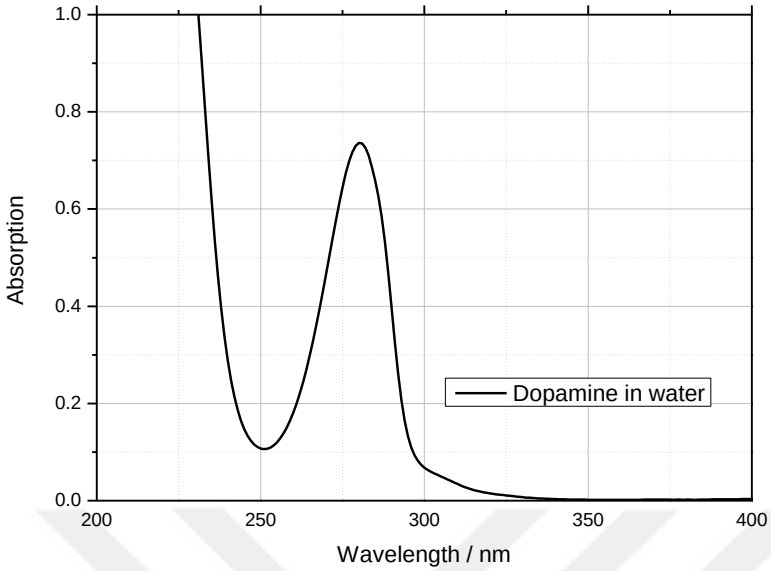

Figure 4.19. UV/Vis absorption spectrum of $1x10^{-4}$ M dopamine in water.

Dopamine has strong fluorescence having maximum wavelength at 320 nm (Fig. 4.20. excitation wavelength 285 nm).

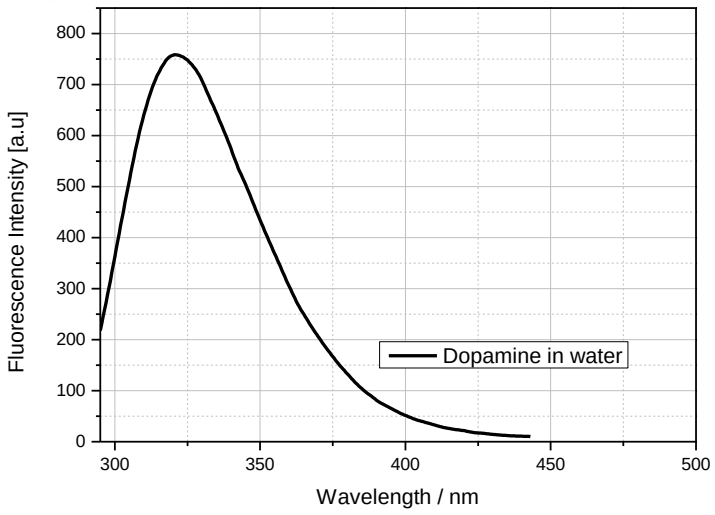

Figure 4.20. Fluorescence spectrum of $4.00x10^{-5}$M dopamine in water λ_{ex}=285 nm.

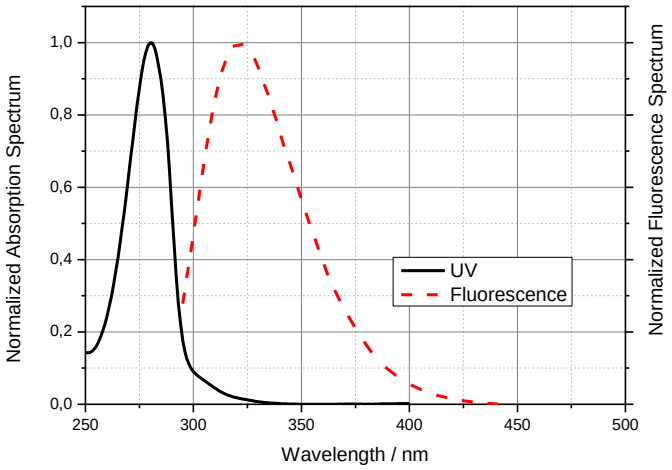

Figure 4.21. Normalized absorption and fluorescence spectrum of dopamine in water

Normalized absorption and fluorescence spectra of dopamine in water was shown in Fig. 4.21. Resonance wavelength was found from the spectra at E_{00} = 294 nm (4.21 eV).

4.2.3 Serotonin (SE)

Serotonin displays a peak at 276 nm in water (Figure 4.22). Additionally, a shoulder is observed at 297 nm (Figure 4.23).

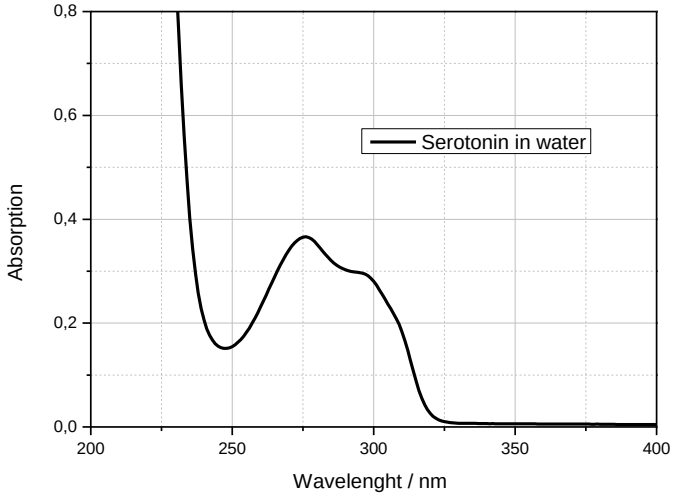

Figure 4.22. UV/Vis absorption spectrum of 4.51x10 $^{-5}$M serotonin in water.

Serotonin at 2.00x10^{-5}M in water has strong fluorescence having maximum wavelength at 340 nm (Fig. 4.18, excitation wavelength 275 nm).

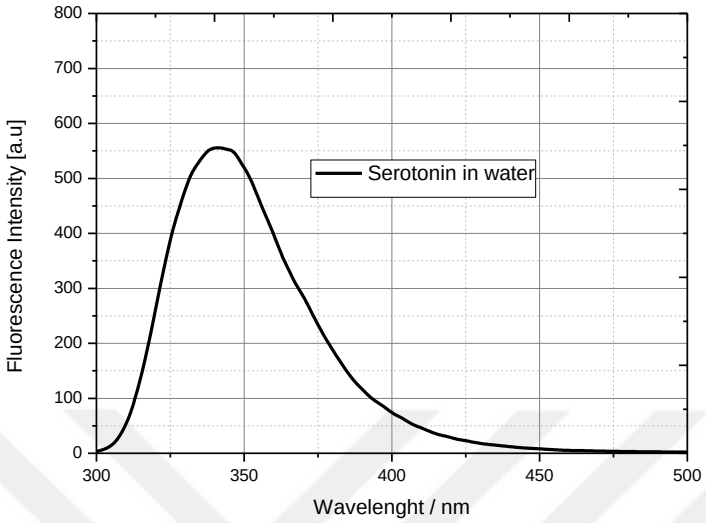

Figure 4.23. Fluorescence spectrum of 2.00x10 $^{-5}$M serotonin in water λ_{ex}=275 nm.

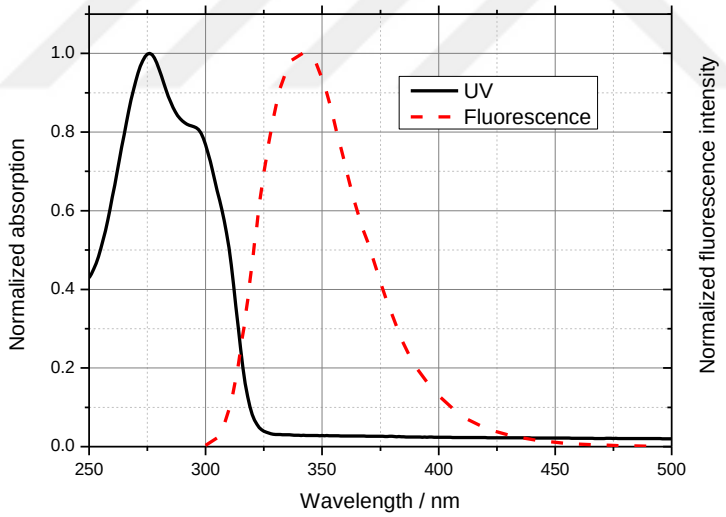

Figure 4.24. Normalized absorption and fluorescence spectrum of serotonin in water.

Normalized Absorption and Fluorescence Spectra of Serotonin in water was shown in Fig. 4.24. Resonance wavelength was found from the spectra at 315 nm (E_{00} = 315nm (3.93 eV)).

4.2.4 Melatonin (MT)

Melatonin displays a peak at 294 nm, the others electronically excited state show up at about 277 nm 222nm in water (Figure 4.25).

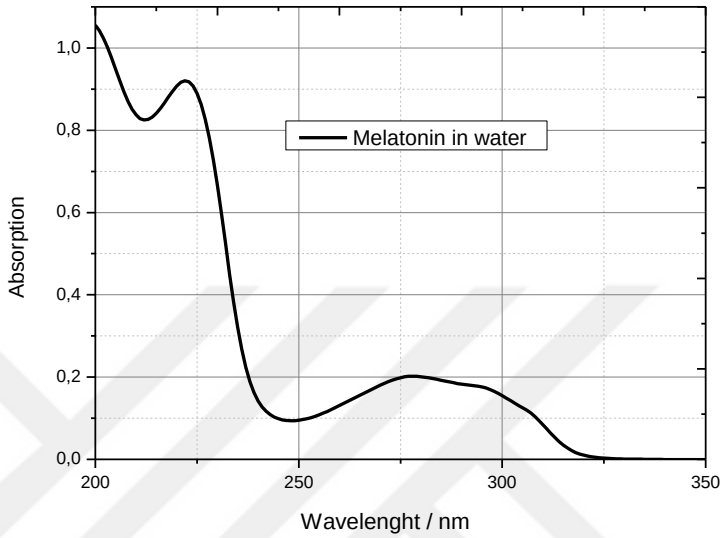

Figure 4.25. UV/Vis absorption spectrum of 6.00×10^{-4}M melatonin in water.

Melatonin at 2.00×10^{-5}M in water has strong fluorescence having maximum wavelength at 367 nm (Fig. 4.26, excitation wavelength 330 nm).

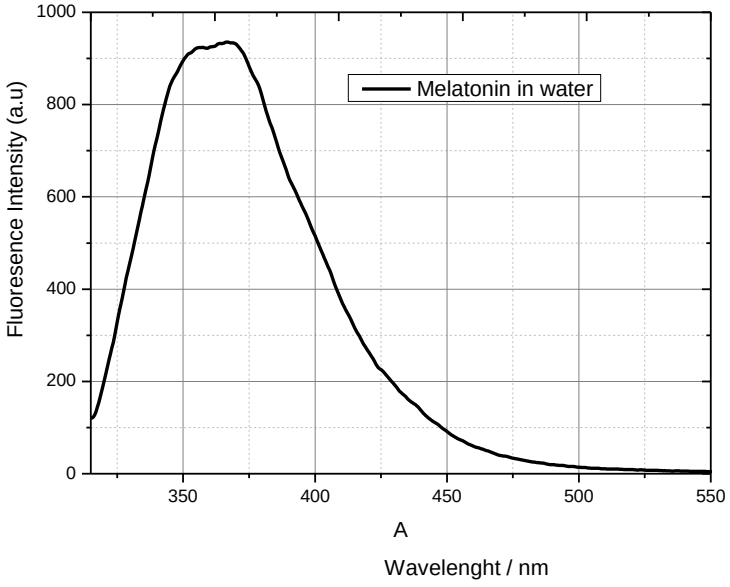

Figure 4.26. Fluorescence spectrum of 2.00×10^{-5} M melatonin in water λ_{ex}=330 nm.

Normalized Absorption and Fluorescence Spectra of Melatonin in water was shown in Fig. 4.27. Resonance wavelength was found from the spectra at E_{00}=318 nm (3.850 eV).

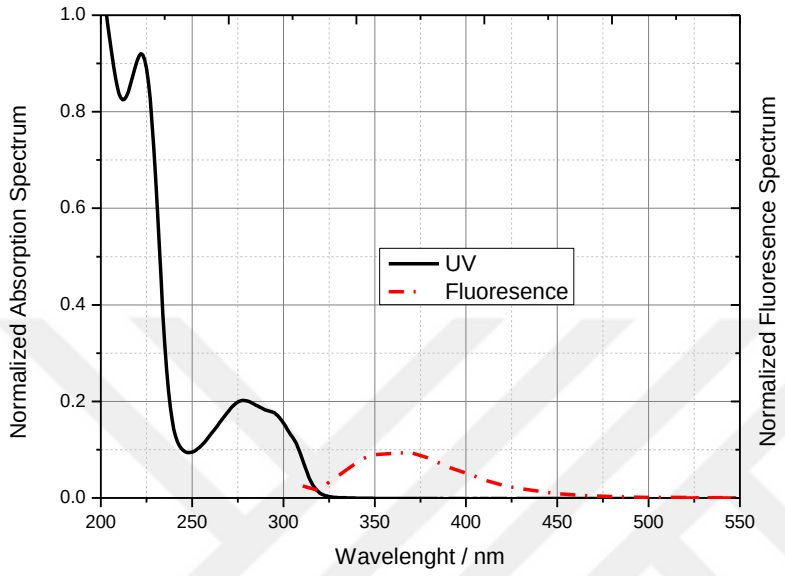

Figure 4.27. Normalized absorption and fluorescence spectrum of melatonin in water E_{00}=318 nm.

4.2.5 Promazine-dopamine (PZ-DA)

UV/Vis absorption spectrum (Figure 4.28) belonging mixture of promazine-dopamine in water is observed. In measurement, when concentration of promazine ($4.00x10^{-5}$ M) is fixed, concentration of dopamine has been increased. The peak of dopamine at 278 nm and the peak of promazine at 250 nm are observed. The peak of promazine at 302 nm is disappeared with dopamine addition.

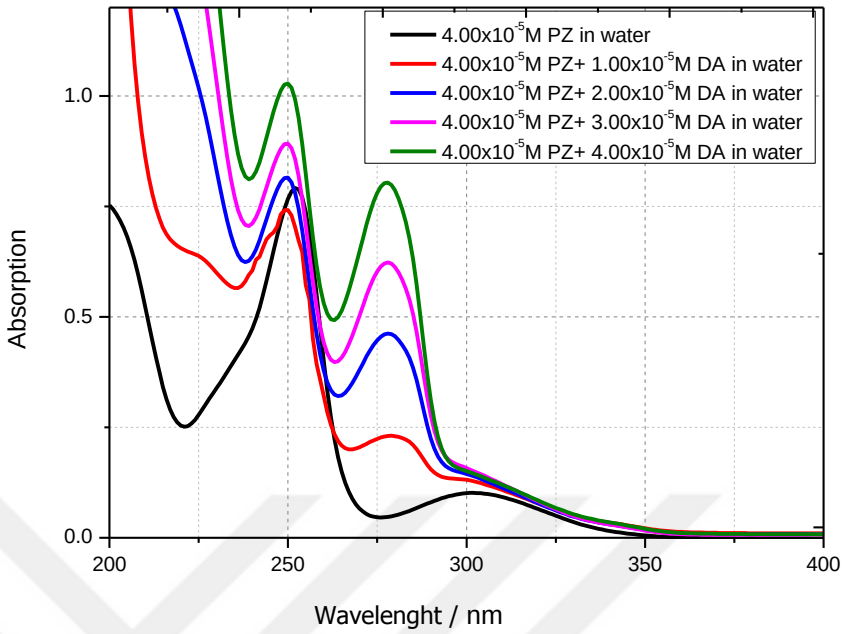

Figure 4.28 UV/Vis absorption spectra of dopamine-promazine system in water.

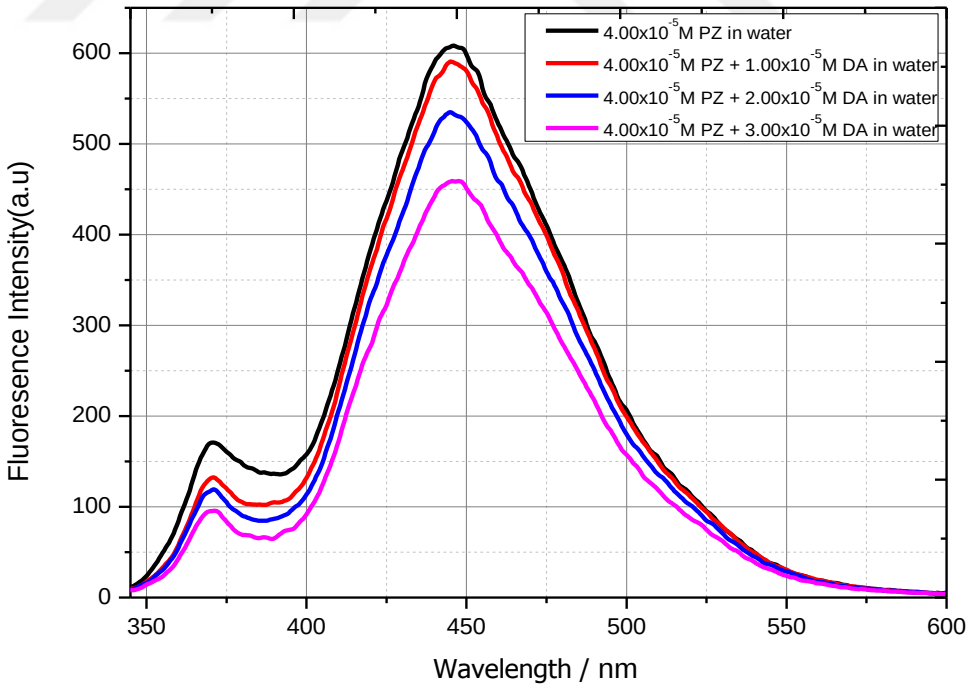

Figure 4.29. Fluorescence spectrum of dopamine-promazine system in water. λex =340

The fluorescence spectrum of promazine-dopamine system in water is observed in the figure 4.29 (λ_{ex} =340). During these measurements of dissolved oxygen in solution to remove nitrogen from samples is overviewed. In this way the fluorescence quenching caused by oxygen clear has been eliminated.

4.00x10^{-5} M concentration alone in water promazine fluorescence spectra was taken (Figure 4.17). Promazine concentrations constant and varying the concentration of solution was prepared by the addition dopamine (Figure 4.29). In the fluorescence spectra is used the same excitation wavelength (λ_{ex} =340) and conditions. Although concentration of promazine dopamine monomer peak decreased by increasing dopamine concentration was observed. Quenching of the fluorescence with increasing concentration of dopamine, in the excited state the interaction between promazine and dopamine is indicated.

.

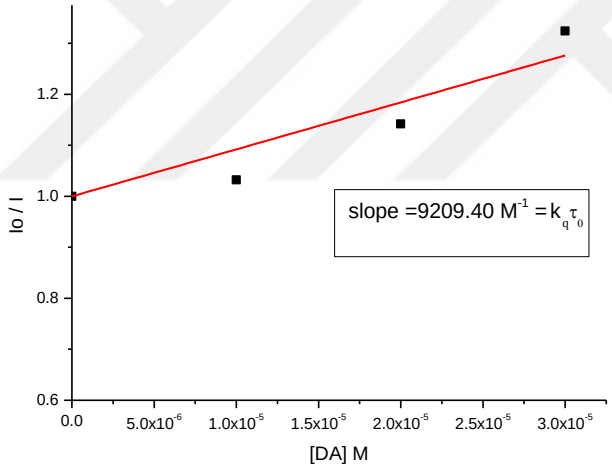

Figure 4.30. Stern Volmer graph of dopamine-promazine system in water.

Stern-Volmer graph for PZ-DA system at 446 nm. Stern-Volmer constant Ksv = 9209.40 M^{-1} was calculated by using Stern-Volmer equation (1.22) from the fluorescence intensities.

Change in Gibbs free energy for electron transfer is calculated using Rehm-Weller equation (1.22). Oxidation potential of dopamine is used as 0.24 V vs SCE (Meng-Meng L. Et al, 2015), and of Promazine is used as 0.58 V vs SCE (Dryhurst G. Et al, 1982) under same conditions. E_{00} value for promazine has

been calculated as 3.54 eV from experimental data; thus its ΔG value in water is calculated as given below:

$$\Delta G = 0.24 - (-0.58) - 3.54 = -2.72 \text{ eV}$$

4.2.6 Promazine-serotonin (PZ-SE)

UV/Vis absorption spectrum (Figure 4.23) belonging mixture of promazine-serotoninin water is observed. In measurement, when concentration of promazine ($4.00x10^{-5}$ M) has been fixed, concentration of serotonin has been increased. Peaks of promazine are seen at 252 nm and 302 nm. Depending to increasing of serotonin concentration, increasing of the peak intensity is observed. Shift was not observed the peaks due to complex in basis state did not occur.

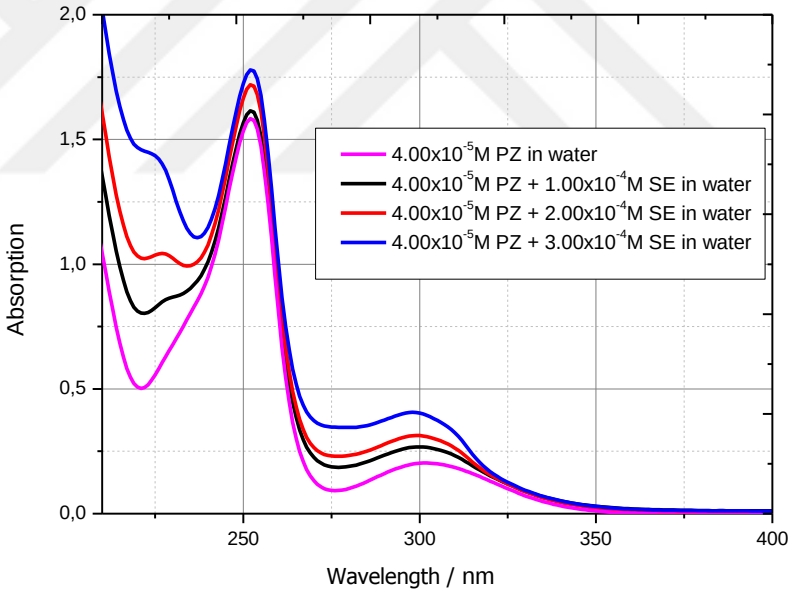

Figure 4.31. UV/Vis absorption spectra of promazine-serotonin system in water.

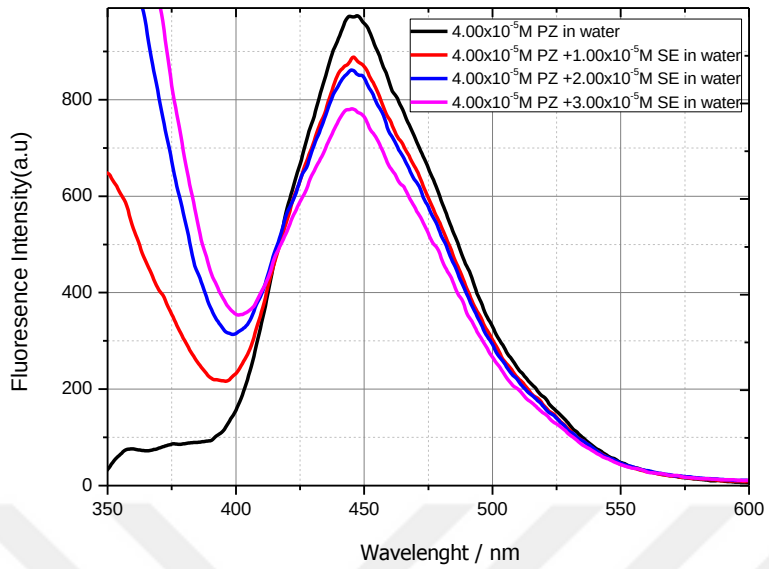

Figure 4.32. Fluorescence spectrum of of promazine-serotonin system in water.

λ_{ex} = 330 nm

Fluoresence spectra of promazine and systems are shown in Figure 4.32. Promazine concentrations constant and varying the concentration of solution was prepared by the addition serotonin (Figure 4.32). The excitation wavelength for promazine-serotonine system is selected as 330 nm. Vibration alone is promazine fluorescence has been fading in the presence of peaks serotonin. While serotonin peaks in about 400 nm is increased, decreasing premarin serotonin monomer peak in 445 nm is observed. Quenching of the fluorescence with increasing concentration of serotonin, in the excited state the interaction between promazine and serotonin is indicated. Saving the intermolecular fluorescence quenching that is encouraging an interaction.

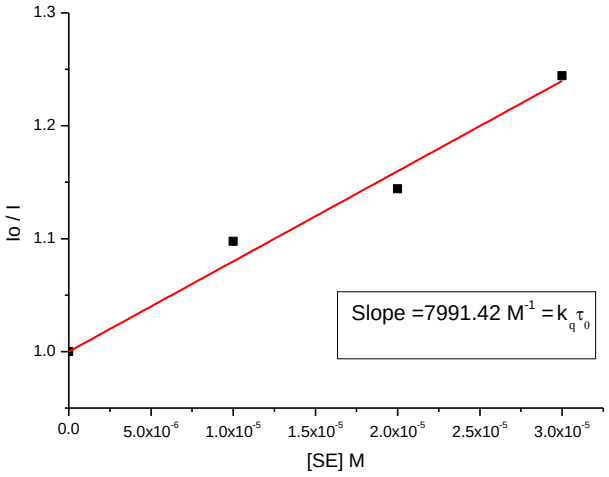

Figure 4.33. Stern Volmer graph of promazine-serotonin system in water.

Stern-Volmer graph for PZ-SE system at 446 nm has been shown in figure 4.33. Stern-Volmer constant Ksv = 7991.42 M^{-1} was calculated by using Stern-Volmer equation (1.22) from the fluorescence spectra of the system.

Change in Gibbs free energy for electron transfer is calculated using Rehm-Weller equation (equation 1.22). Oxidation potential of serotonin is used as 0.33 V vs SCE (Gusphyl A. J. et al, 2006), and of promazine is used as 0.58 V vs SCE (Dryhurst G. Et al, 1982) under same conditions. E_{00} value for promazine has been calculated as 3.54 eV from experimental data; thus its ΔG value in water is calculated as given below:

$$\Delta G = 0.33 - (-0.58) - 3.54 = -2.63 \text{ eV}$$

4.2.7 Promazine-melatonin (PZ-MT)

Promazine also keep the fixed concentration 4,00x10^{-5}M, melatonin concentration in the water is increased in the UV/Vis absorption spectrum. As we know that promazine peaks are at 302 nm and 252 nm, the peak at 302 nm is showed blue shift until 297 nm. At 277 nm characteristic transition peak of melatonin was dissappering in all cases. In this case n-π* complex in the ground state has been formed.

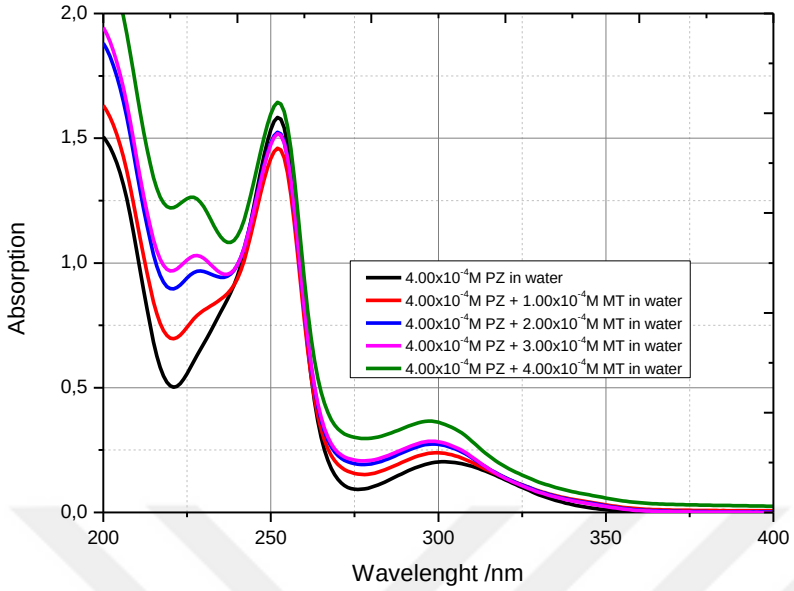

Figure 4.34. UV/Vis absorption spectra of melatonin-promazine system in water.

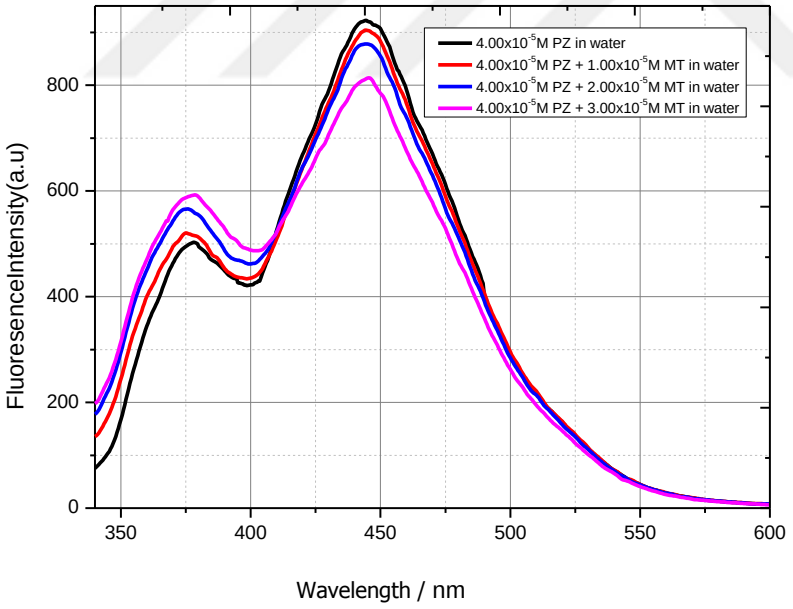

Figure 4.35. Fluorescence spectrum of of melatonin-promazine system in water λ_{ex}=330 nm.

Promazine the characteristic peak (445 nm) and melatonin the characteristic peak (367 nm) is seen. Promazine concentrations constant and varying the concentration of solution was prepared by the addition melatonin. Despite of

increasing concentration of melatonin, decreasing of promazine-melatonin monomer peak (444 nm) is observed (Figure 4.35). The peak intensity increases with increasing melatonin concentration at 375. Quenching of the fluorescence with increasing concentration of melatonin at 444 nm and incresing peak intensity at 375 nm in the excited state shows the interaction between promazine and melatonin is indicated. Considering that ground state complex is stimulated in excitation wavelength at 345 nm, we can say that the shifting of fluorescence peaks and quenching in complex result from the formation.

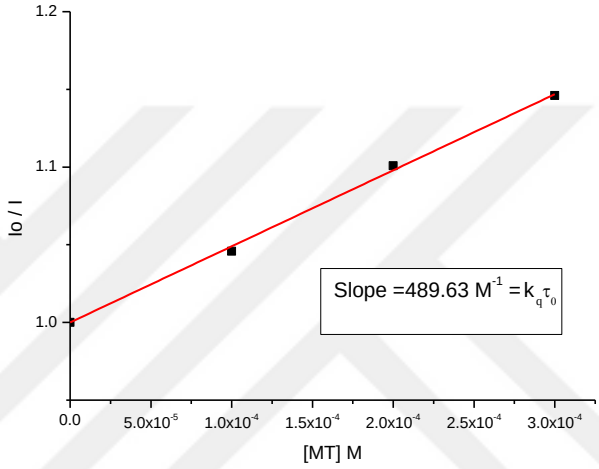

Figure 4.36. Stern Volmer graph of melatonin-promazine system in water.

Figure 4.36 shows Stern-Volmer graph for PZ-MT system at 446 nm. Stern-Volmer constant Ksv = 489.63 was calculated by using Stern-Volmer equation (1.14) from the measured fluorescence intensities.

5. CONCLUSION

Complexes between Promazin and Dopamine/ Serotonin/ Melatonin investigated by computationally and experimentally. In computational part, both HOMO and LUMO are located mostly on the rings for all studied monomers. The results displayed for promazine and the hormones (Dopamine, Serotonin and Melatonin) indicated that there were no significant changes in the properties and molecular orbitals in gas phase and in water. Also, charge transition was easier in water than in gas phase. All complexes had different geometries in gas phase and in water. The charge transfer from donor (hormonos) to promazine (CT2) was observed at $S_0 \rightarrow S_1$ transition in all systems in gas phase and in water (Table 5.1). The only exception is the PZ-DA system in gas phase where CT2 was observed at $S_0 \rightarrow S_3$ transition instead of $S_0 \rightarrow S_1$. It is clearly seen that charge transfer increases significantly at higher transitions in gas phase. In contrast to gas phase, the $S_0 \rightarrow S_1$ transition corresponds to charge transfer from dopamine to promazine (CT2) accompanied by a locally excited promazine (LE1) in water. In all other transitions except $S_0 \rightarrow S_3$ charge transfer is the main process, but $S_0 \rightarrow S_3$ transition has been mostly dominated by locally excited promazine (LE1) and dopamine (LE2).

The $S_0 \rightarrow S_1$ transition is a mixture of charge transfer from promazine to serotonin (CT1), charge transfer from serotonin to promazine (CT2), locally excited promazine (LE1), and locally excited serotonin (LE2). It may be concluded that promazine-serotonin system has a tendency for charge transfer in gas phase in contrast to the promazine-dopamine system. The $S_0 \rightarrow S_1$ transition is a mixture of charge transfer from melatonin to promazine (CT2), locally excited promazine (LE1), and locally excited melatonin (LE2) in gas phase. The main contribution comes from H-2→L (62%) which corresponds to CT2+LE1. It may be concluded that promazine-melatonin system has a tendency for charge transfer in gas phase similar to promazine-serotonin system but in contrast to the promazine-dopamine system. In water, $S_0 \rightarrow S_1$ transition has only CT2 character. The main transition from H-1→L corresponds to CT2 (64%).

Experimentally, characteristic UV/Vis absorption spectra of molecules were protected in all systems. This shows that complex in ground state did not form. PZ-DA system has the largest Stern-Volmer constant (K_{SV}) among all studied

systems. On the other hand, electron transfer energy (ΔG) is more negative than that of serotonin system. This result may indicate that PZ-DA system has more tendency to form a complex in water compared to the other studied systems. Current results show that all investigated systems have potential to be used in photosensetive material design. Although dopamine system seems more appropriate for those designs, it should be noted that promazine will go to the excited state together with dopamine.

Table 5.1. Main electronic transitions and corresponding wavelengths for the studied compounds and their complexes

Molecules	**CALCULATED**				**EXPERIMENTAL**	
	in gas phase		in water		in water	
	transition	λ (nm)	transition	λ (nm)	λ_{max} (nm)	λ_{fluo} (nm)
PZ	$S_0 \rightarrow S_1$	283	$S_0 \rightarrow S_1$	284	302	446
DA	$S_0 \rightarrow S_1$	240	$S_0 \rightarrow S_1$	240	280	320
SE	$S_0 \rightarrow S_1$	259	$S_0 \rightarrow S_1$	260	276	342
MT	$S_0 \rightarrow S_1$	259	$S_0 \rightarrow S_1$	259	277	370
PZ-DA	$S_0 \rightarrow S_1$	306 (LE)	$S_0 \rightarrow S_1$	286 (LE+CT)	278 (DA) 250 (PZ)	370 446
	$S_0 \rightarrow S_3$	262 (LE+CT)	$S_0 \rightarrow S_3$	260 (LE+CT)		
PZ-SE	$S_0 \rightarrow S_1$	290 (LE+CT)	$S_0 \rightarrow S_1$	295 (CT)	252 (PZ) 302 (PZ)	446
PZ-MT	$S_0 \rightarrow S_1$	281 (CT)	$S_0 \rightarrow S_1$	283 (CT)	252 (PZ) 302 (PZ) 297 (CT)	375 444

CT: charge transfer from hormons to promazine, LE: locally excited promazine

REFERENCES

Albery W.J., Foulds A.W., Hall K.J., Hillman A.R., Edgell R.G., and Orchard A.F., 1979, Nature, 282, 793.

Armaroli N., and Balzani V., 2011,Energy for sustainable world from the oil age to a sun-powered future, Wiley-VCH, Weinheim ch.,11p.

Bernsmann F., Ersen O., Voegel J. C., Jan E., Kotov N. A., and Ball V., 2010, ChemPhysChem 11, 3299-3305.

Bloor J.E., and Med J. , 1970, Chem., 13, 922.

Chattopadhyay A., Rukmini R., and Mukherjee S., 1996, Biophys. J., 71, 1952-1960pp.

Cogordan J. A., Mayoral M., Angeles E., Toscano R. A., and Martinez R., 1999, International Journal of Quantum Chemistry, 71, 415-432.

Daniel W. A., 2003, Progress in Neuro-Psychopharmacology & Biological Psychiatry, 27, 65–73.

Daniel W.A., Syrek M., and Wo´jcikowski J., 1999, Eur. Neuropsychopharma. 9, 337–344pp.

Darvesh S., Macdonald I. R., and Martin E., 2013, Bioorganic & Medicinal Chem. Lett., 23, 3822–3825.

Dennington Roy, Keith Todd, and Millam John, 2009, GaussView, Version 5, Semichem Inc., Shawnee Mission, KS.

Dryhurst G., Kadish K. M., Scheller F., and Renneberg R., 1982, Biologıcal electrochemıstry, volume I, Academic Press, New York, London, 209-259.

Eghbal M.A., Tafazoli S., Pennefather P., and O'Brien P.J., 2004, Chem. Biol. Interact., 151, 43–51.

Förster T., and Kasper K., 1955, Z. Phys. Chem. N.F., 59,10, 976.

Franck J., 1926, Transactions of the faraday society, 21, 536–542; Condon, E., 1926, Physical Review, 28, 1182–1201.

Frisch M. J.; Trucks G. W., Schlegel H. B., Scuseria G. E., Robb M. A., Cheeseman J. R., Scalmani G., Barone V., Mennucci B., Petersson G. A., Nakatsuji H., Caricato M., Li X., Hratchian H. P., Izmaylov A. F., Bloino J., Zheng G., Sonnenberg J. L., Hada M., Ehara M., Toyota, K.;

REFERENCES (continue)

Fukuda R., Hasegawa J., Ishida M., Nakajima T., Honda Y., Kitao O., Nakai H., Vreven, T., Montgomery J. A. Jr., Peralta J. E., Ogliaro F., Bearpark M., Heyd J. J., Brothers E., Kudin K. N., Staroverov V. N., Kobayashi R., Normand J., Raghavachari K., Rendell A., Burant J. C., Iyengar S. S., Tomasi J., Cossi M., Rega N., Millam J. M., Klene M., Knox J. E., Cross J. B., Bakken V., Adamo C., Jaramillo J., Gomperts R., Stratmann R. E., Yazyev O., Austin A. J., Cammi R., Pomelli C., Ochterski J. W., Martin R. L., Morokuma K., Zakrzewski V. G., Voth G. A., Salvador P., Dannenberg J. J., Dapprich S., Daniels A. D., Farkas Ö., Foresman J. B., Ortiz J. V., Cioslowski J., and Fox D. J., 2009, Gaussian, Inc., Wallingford CT.

Guo L., Zhang Y., and Li Q., 2009, Analy. Sciences, 25, 1451-1455.; **Zafar K. S., Siegel D., and Ross D.,** 2006, Mol. Pharma. 70, 3, 1079-1086; **Mohammad-Shiri H., Ghaemi M., Riahi S., and Akbari-Sehar A.,** 2011, Int. J. ELectrochem. Sci., 6, 317-336.

Gusphyl A. J., Mingui S., Yingze Z., and Tracy Cui X., 2006, Proceedings of the 28th IEEE, EMBS Annual International Conference, New York City, USA, 4115- 4118.

Harusuke A., Naoto N., Yuji O., Hideo Y., and Nobumasa K., 1998, Neuroscience Letters, 252, 91–94.

Imabayashi S., Ban K., Ueki T., and Watanabe M., 2003, J. Phys. Chem. B, 107, 8834.

Jablonski A., 1933, Nature, 131, 839-840.

Kavarnos G. J., 1993, Fundamentals of photoinduced electron transfer, VCH Publisher, New York, 359p.

Kim G.W., Cho M.J., Yu Y.J., Kim Z.H., Jin J.I., Kim D.Y., and Choi D.H., 2007, Chem. Mater., 19, 42.

Klanp.Wirz J., 2009, Photochemistry of organic compound, Wiley New York.

Knibbe H., Röllig K., Schäfer F. P., and Weller, A., 1967, J. Chem. Phys., 47, 1184-1185pp.

REFERENCES (continue)

Kohn W., and Sham L. J., 1965, Phys. Rev., 140, A1133.

Kuzmin M. G., 1993, Pure and Applied Chemistry, 65(8), 1653-1658pp.

Lakowicz J. R., 1999, Principles of fluorescence chemistry, Plenum Press, New York and London, 510p.

Leonhardt H., and Weller, 1961, A., Z. Phys. Chem. N.F., 29, 277.

Levine I. N., 1991, Quantum Chemistry, Printice-Hall, New Jersey.

Lippert E., 1957, Z. Elektrochem., 61, 962.

López Sastre J. A., Miguel R. N., Molina R. P., Zarzuelo M. C. G., Romero-Avila C., and Ramos A. G., 2001, J. Mol. Struc.(Theochem), 537, 271-281pp.

Mataga N., Kaifu Y. and Koizumi M., 1956, Bull. Chem.Soc. Jpn, 29, 465.

Mataga N., Kaifu Y., and Koizumi, M., 1955, Nature, 175, 731.

Meng-Meng L., Shu-Min H., Xiao-Wen Z., Ling-Li H., Tao L., and Zhang-Yu Y., 2015, Int. J. Electrochem. Sci., 10, 235 – 247.

Monzon L.M.A., and Yudi L.M., 2008, Electrochimica Acta, 53, 2217–2225.

Morrist A. J., Meyer G. J. and Fujita E., 2009, Molecular approaches to the photocatalytic reduction of carbon dioxide for solar, Acc. Chem. Res.42,12, 1983–1994 pp.

Mulliken R. S., 1952, J. Am. Chem. Soc. 74, 811.

Nashed R., 2013, J Renew. Sustain. Energy, 5,2, 022701.

Onsager L., 1931, Phys. Rev. , 37, 405 - Ibid., 1931, 38, 2265.

Orbach N. and Ottolenghi M., 1975, Chem.Phys. Lett., 35(2), 175-180pp.

Pan D., Shoute L. C. T., and Phillips D. L., 1999, J. Phys. Chem. A 103, 6851-6861.

Potashnik R., Goldschmidt C. R., Ottolenghi M., and Weller, A., 1971, J. Chem. Phys., 971, 5344-5348pp.

Raghupathy E., Peterson N. A., and McKean C. M., 1970, Biochem. Pharma., 19, 993-1000.

REFERENCES (continue)

Shen X., 2013, Electrochem. Comm., 30, 13-16.

Spartan Molecular Database, 2008, Wavefunction, Inc. Irvine, CA 92612 USA.

Takada T., Kawai K., Fujitsuka M., and Majima T., 2006, J. Am. Chem. Soc., 128, 11012.; **Weiss E.A., Ahrens M.J., Sinks L.E., Ratner M.A., and Wasielewski M.R.**, 2004, J. Am. Chem. Soc., 126, 9510.

Takashi Y., Jan K., Shimako Y., Kaoru F., Hitoshi N. and Masatoshi Y., 2004, Journal of Chromatography B, 807, 177-183.

Thrower J.D., 2013, J. Phys. Chem. C, 117, 13520-13529.

Turro N. J., Ramamurthy V, and Scaiano J. C., 2010, Modern molecular photochemistry of organic molecules, University Science Books, Sausalito.

Wainwright M., Mohr H., and Walker W.H., 2007, J. Photochem. photobiol. B, 86, 45–58.; **Nagy S., Argyelan G., Molnar J., Kawase M., and Motohashi N.,** 1996, Anticancer Res., 16, 1915–1918.

Weller A., 1961, Progress in reaction kinetics I, G. (Ed), Pergamon Press, 276, New York, Oxford, London, Paris, 189-214.

CURRICULUM VITAE

Name Surname : Tuğçe Şener

Profession : Chemist

Date / Place of Birth : 1988 / Muğla

Nationality : Turkish

Sex : Female

Adress : Ege University, Faculty of Science,
Department of Chemistry,
Division of Physical Chemistry, 35100
Bornova-Izmir / Turkey

E-mail : tgcsener@gmail.com

EDUCATIONAL BACKGROUND

B.S In Chemistry, 2012, Anadolu University, Eskişehir-Turkey